AD NUMBER

AD922519

NEW LIMITATION CHANGE

TO

Approved for public release, distribution unlimited

FROM

Distribution authorized to U.S. Gov't. agencies only; Test and Evaluation, Apr 1974. Other requests shall be referred to AFAL/TEL, Wright-Patterson AFB, OH 45433.

AUTHORITY

Per AFAL, Wright-Patterson AFB, OH

AFAL-TR-74-17

AD922519

ADVANCED MODULATOR II

J.R. Teague and L.B. Allen
MCDONNELL DOUGLAS ASTRONAUTICS COMPANY–EAST
MCDONNELL DOUGLAS CORPORATION
ST. LOUIS, MO. 63166

16 MAY 1974

TECHNICAL REPORT AFAL-TR-74-17

Prepared For

AIR FORCE AVIONICS LABORATORY
AIR FORCE SYSTEMS COMMAND
WRIGHT-PATTERSON AIR FORCE BASE, OHIO 45433

NOTICES

When Government drawings, specifications, or other data are used for any purpose other than in connection with a definitely related Government procurement operation, the United States Government thereby incurs no responsibility nor any obligation whatsoever; and the fact that the Government may have formulated, furnished, or in any other way supplied the said drawings, specifications, or other data, is not to be regarded by implication or otherwise as in any manner licensing the holder or any other person or corporation, or conveying any rights or permission to manufacture, use, or sell any patented invention that may in any way be related thereto.

Copies of this report should not be returned unless return is required by security considerations, contractual obligations, or notice on a specific document.

UNCLASSIFIED

SECURITY CLASSIFICATION OF THIS PAGE *(When Data Entered)*

REPORT DOCUMENTATION PAGE		READ INSTRUCTIONS BEFORE COMPLETING FORM
1. REPORT NUMBER AFAL TR-74-17	2. GOVT ACCESSION NO.	3. RECIPIENT'S CATALOG NUMBER
4. TITLE *(and Subtitle)* ADVANCED MODULATOR II		5. TYPE OF REPORT & PERIOD COVERED Final Report for Period 22 Mar 73 - 12 Nov 73 6. PERFORMING ORG. REPORT NUMBER
7. AUTHOR(s) J. R. Teague and L. B. Allen		8. CONTRACT OR GRANT NUMBER(s) F33615-73-C-1144
9. PERFORMING ORGANIZATION NAME AND ADDRESS McDonnell Douglas Astronautics Company - East St. Louis, Missouri 63166		10. PROGRAM ELEMENT, PROJECT, TASK AREA & WORK UNIT NUMBERS 400-06-10
11. CONTROLLING OFFICE NAME AND ADDRESS Air Force Avionics Laboratory Air Force Systems Command Wright-Patterson AFB, Ohio 45433		12. REPORT DATE ~~12 January 1974~~ 16 May 1974 13. NUMBER OF PAGES 46
14. MONITORING AGENCY NAME & ADDRESS *(if different from Controlling Office)*		15. SECURITY CLASS. *(of this report)* Unclassified 15a. DECLASSIFICATION/DOWNGRADING SCHEDULE

16. DISTRIBUTION STATEMENT *(of this Report)*

Distribution is limited to U.S. Government Agencies only, test and evaluation data; April 1974. Other requests for this document must be referred to AFAL/TEL, Wright-Patterson AFB, Ohio 45433.

17. DISTRIBUTION STATEMENT *(of the abstract entered in Block 20, if different from Report)*

18. SUPPLEMENTARY NOTES

19. KEY WORDS *(Continue on reverse side if necessary and identify by block number)*

1 Gbps PGBM Laser Communications Subsystem, Mode-Locked and Frequency Doubled Nd:YAG Laser, Optical Modulator, Lithium Tantalate

20. ABSTRACT *(Continue on reverse side if necessary and identify by block number)*

The objective of this program was to conduct exploratory development of a 1 Gbps single-pass single-unit (unmultiplexed) modulator for use with a mode-locked and frequency-doubled neodymium YAG laser in a space laser communication system. The modulator was to operate at data rates up to 1 Gbps and be able to handle 0.53 micrometer laser power up to 0.25 watts while maintaining its specified operating characteristics. The performance goals were (1) a static extinction ratio of 100 to 1 or greater, (2) a worst

DD FORM 1 JAN 73 1473 EDITION OF 1 NOV 65 IS OBSOLETE

UNCLASSIFIED

SECURITY CLASSIFICATION OF THIS PAGE *(When Data Entered)*

20. ABSTRACT. (Continued)

case dynamic extinction ratio of 30 to 1 or greater with a 1 Gbps pseudorandom code input, (3) 100% depth of modulation, and (4) at least 80% transmission of the beam input power statically. This effort was to develop a 1 Gbps 0.53 micrometer modulator and driver in breadboard form to be used as a laboratory tool to demonstrate the feasibility of this modulator design concept.

The modulator development utilized lithium tantalate crystals in four different configurations. The modulator drivers were designed with both thin film hybrid and discrete component input stages with the dual output stage using only discrete components. Various modulator and modulator driver combinations were used in the dynamic performance evaluations.

The performance of the best modulator and modulator driver met most of design goals. The modulator driver had 20 volts ± 1 volt outputs with timing inaccuracies of $\leq \pm$ 175 ps including PN generator timing inaccuracies of $\leq \pm$ 70 ps. The driver had rise times between 400 ps and 500 ps. The modulator had two 10mm long lithium tantalate crystals tapered in the c-axis in order to reduce the switching voltage by 20% which resulted in a dc half-wave switching voltage of 19.8 volts at 0.53 μm wavelength. This modulator had a static extinction ratio of 90:1 and a worst case dynamic extinction ratio of $\geq$ 22.4:1 with a 1 Gbps pseudorandom code. The depth of modulation was 100% since the driver applied full half-wave switching voltage to the modulator. The modulator (crystals only - single pass) transmitted 81.5% of the beam input power statically.

FOREWORD

This report was prepared by the McDonnell Douglas Astronautics Company-East, McDonnell Douglas Corporation, St. Louis, Missouri, under Contract F33615-73-C-1144, Project No. 405B. This report covers the period of 15 March 1973 through 15 October 1973 and is the Final Report on this contract. The work described herein was carried out by the Advanced Electronic Techniques Department at the McDonnell Douglas Astronautics Company-East, Box 516, St. Louis, Missouri 63166.

Dr. L. B. Allen of McDonnell Douglas was Project Engineer. Dr. J. R. Teague was the major contributor to the program. Dr. V. H. Nettle designed and built the modulator drivers. All of these contributors received technical direction from A. L. Furfine (Department Manager), R. A. Stacy (Branch Manager), and M. Ross (Manager of Laser Technology) in the MDAC-East organization. The report was submitted by the authors on 15 November 1973.

TABLE OF CONTENTS

LIST OF FIGURES

LIST OF FIGURES (CONTINUED)

LIST OF TABLES

1. INTRODUCTION AND PROGRAM SUMMARY

The objective of this program was to conduct exploratory development of a 1 Gbps single-pass single-unit (unmultiplexed) modulator for use with a mode-locked and frequency-doubled neodymium YAG laser in a space laser communication system. The exploratory effort was directed toward the investigation and solution of problems for Pulse Gated Binary Modulation (PGBM) modulator operation. The modulator was to operate at data rates up to 1 Gbps and be able to handle 0.53 micrometer laser power up to 0.25 watts while maintaining its specified operating characteristics. The performance goals were (1) a static extinction ratio of 100 to 1 or greater, (2) a worst case dynamic extinction ratio of 30 to 1 or greater with a 1 Gbps pseudorandom code input, and (3) a static optical transmission of at least 80%. This effort was to develop the Gbps 0.53 micrometer modulator and provide a driver in breadboard form to be used as a laboratory tool to demonstrate the feasibility of the 1 Gbps modulator design concept. Several breadboard modulator-driver combinations were fabricated and evaluated. No hardware delivery was required.

The four modulator units developed and evaluated under this program used the baseband and digital Pulse Gated Binary Modulation (PGBM) format. In the PGBM format, pulses emitted by a mode-locked laser are either transmitted by the modulator to represent a logic "1" or blanked by the modulator to represent a logic "0". Each modulator unit employed high quality lithium tantalate crystals in a crossed axis single-pass arrangement. The crystals were individually matched into a broadband 50 ohm impedance network. The modulators were driven by dual output solid state drivers. The crystals were packaged in an oven which was operated at 150°C to prevent optical damage and to reduce the crystal switching voltage. Each of the modulators and an appropriate driver was set up in a test bed and evaluated. The performance of each of the four modulators developed and evaluated during this program is summarized in Table 1.

The two 10 mm straight crystal modulator, (AM #1) which required 24 volts for full half-wave switching, was operated with the driver having thin film hybrid input stages with discrete components in the dual output stage (MD-2-003). The driver had 18 volts output with timing inaccuracies $\leq \pm$ 200 ps. The modulator had 80% optical tranmission and a static extinction ratio of 17 dB. The worst case dynamic extinction ratio was $\geq$ 17.5:1; however, the "ones" level was only 80% full amplitude due to the low driver output voltage.

The four 7 mm straight crystal modulator (AM #2), which had a half-wave switching voltage of 17 volts, was operated with the thin film hybrid input stage drivers, MD-2-002 and MD-2-003 having respectively 17 volt and 18 volt outputs and each having timing inaccuracies of $\leq \pm$ 200 ps. The modulator had 40% optical transmission and a static extinction ratio of 11 dB. The worst case dynamic extinction ratio was $\geq$ 5:1. This modulator had poor static and dynamic extinction ratios because the work strain in the crystals was not removed by etching.

The second two 10 mm crystal modulator (AM #3) was designed with tapered

b-faces on the crystals to reduce their capacitance approximately 20%. This does not affect the switching voltage or the optical transmission, but by reducing the capacitance by one picofared the modulator should have a twenty percent faster rise time. The modulator crystals had mounting strain which limited the static extinction ratio to 14 dB. The worst case dynamic extinction ratio was $\geq$ 7:1. A 24 volt discrete component driver (SSD #4) was used which had a timing inaccuracy of $\leq \pm 350$ ps. The optical transmission was 77%. It was noted that the driver timing inaccuracies were imposing the limitation on the dynamic extinction ratio. No noticeable improvement over the two 10 mm straight crystal modulator (AM #1) was observed with the lower capacitance modulator (AM # 3).

A third two 10 mm crystal modulator (AM #4) was fabricated with the crystals tapered in the c-face in order to lower the half-wave switching voltage. The lower switching voltage should reduce the required driver output voltage so that better timing accuracy could be obtained due to the lower power amplification required per driver stage. The voltage tapered crystal modulator (AM #4) had a half-wave switching voltage of 19.8 volts. The modulator was driven by a discrete component driver (3x) with 20 volts $\pm$ 1 volt output which had timing inaccuracies of $\leq \pm$ 175 ps. The modulator had a static extinction ratio of 90:1 and a worst case dynamic extinction ratio $\geq$ 22.4:1 with a 1 Gbps pseudorandom code input. The modulator transmitted 81.5% of the beam input power. The amplitude of the smallest one in the code was 95.5% of the maximum one transmission; therefore, the transmission of the smallest one was 77.8%. This modulator unit required 24.6 watts of electrical power to drive the modulator to full half-wave switching voltage at 0.53 μm. The performance of this modulator and modulator-driver combination was more completely evaluated than the previously mentioned AM #1, AM #2 and AM #3.

Section II contains a detailed description of each of the modulator units, driver units, and improved modulator components. Performance tests and test results for each modulator are given in Section III. Section IV contains reliabilityand maintainability data applicable to the modulator units evaluated during this contract. Conclusions and recommendations are given in Section V.

TABLE 1 DYNAMIC PARAMETERS FOR $LiTaO_3$ 1 Gbps MODULATOR

MODULATOR NUMBER	DYNAMIC EXTINCTION RATIO	SWITCHING VOLTAGE	MODULATOR DRIVER NUMBER	LASER PULSEWIDTH (10% to 10% Points)	VOLTAGE REFLECTION COEFFICIENT
AM #1	8:1 17.5:1	24V	SSD #4 MD-2-003	300 ps	<4%
AM #2	5:1	17V	MD-2-002 MD-2-003	300 ps	<8%
AM #3	9:1	24V	SSD #4	300 ps	<8%
AM #4	16.3:1 22.4:1	19.8V	MD-2-003 3X	300 ps	<8%

2. MODULATOR DEVELOPMENT

The purpose of the modulator development was to provide a breadboard modulator which when combined with a breadboard driver provided 1 Gbps PGBM modulation of 0.53 μm laser light with performance equal to or better than the performance goals outlined in Section I. Prior to this program we fabricated similar modulator systems for our own use, and for delivery, at 100 Mbps, 300 Mbps, 400 Mbps, and 500 Mbps. Our experience at the lower data rates, especially 500 Mbps, indicated that the same modulator design approach could be used at 1 Gbps with adequate performance. We therefore determined that as few changes in basic mechanical configuration as possible would be made so that it would be possible to fabricate and test at least three separate modulator-driver combinations.

2.1 Mechanical Configuration

Lithium tantalate, furnished GFE by the Air Force Avionics Laboratory, was used as the electrooptic modulator material for all of the modulator fabrication, except where noted. The crystals were always used in pairs. The basic crystal mounting arrangement is shown in Figure 1. The lithium tantalate crystals are oriented so that the polarized laser light travels through the crystals in a direction parallel to the "C" faces. The light enters the crystals polarized at 45° with respect to the crystal axes. In this configuration, the input beam is divided equally into the two polarizations within the crystal, i.e., ordinary (O-wave) and extraordinary (E-wave).

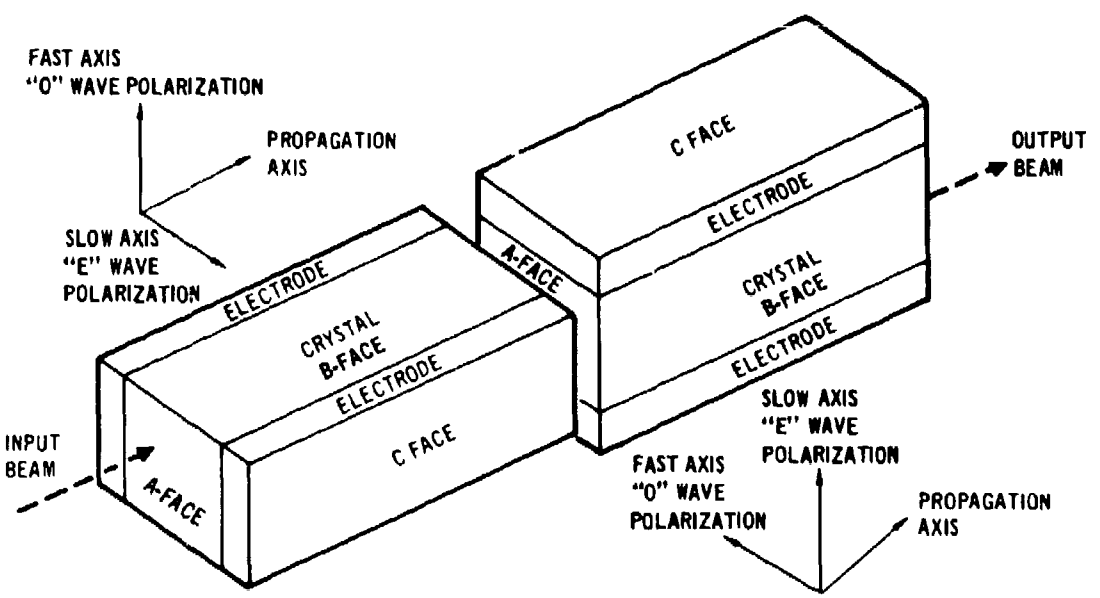

FIGURE 1 CRYSTAL MOUNTING ARRANGEMENT

The two crystals are oriented so that their axes are crossed (as shown in Figure 1). The light which travels as O-wave light in the first crystal travels as E-wave light in the second crystal. Similarly, light which travels as E-wave light in the first crystal travels as O-wave light in the second crystal. One can see that, when the two crystals were identical in length (as they are when cut from a single piece of material), the total optical length traversed by each polarization is identical, provided that the crystals are at the same temperature. In our mounting configuration this crossed axis crystal arrangement provides about two orders of magnitude of cancellation of thermal effects normally present in a single crystal. The phase retardation induced by placing a voltage across the "C" faces is a field distance product. The crystals are therefore made as long and thin as practical, so that the field distance product required to achieve half-wave switching is minimized.

Each of the crystal pairs is placed in a modulator subassembly, shown in exploded form in Figure 2. The modulator subassembly consists of the oven subassembly, and lens holders. The oven subassembly consists of the crystal oven and modulator matching networks. The lens holders provide x, y, and z motion adjustments for the modulator lenses and are lockable in any position. An exploded view of the lens holder is shown on the right hand side of Figure 3. The adjustment motion is produced by a sliding plate. The horizontal adjustment is accomplished by a screw on one side of the sliding plate, with a spring on the other side opposing it. The vertical adjustment works in a similar manner. The lens is held in a cylinder which is a close slip fit into the sliding plate. The lens can be manually pushed in and out for focusing adjustments. The oven body is used for mechanical support and as an isothermal enclosure which thermally stabilizes the modulator interior.

The matching network cables, heater leads, and thermistor leads enter the oven through the base of the oven body which acts as a ground plane for the high frequency modulation drive signals. The oven core is held in place by end bells shaped for maximum support of the oven core and made of teflon to control the oven heat leak, and provide minimal interaction with the modulator matching networks. The oven core is made of boron nitride. Boron nitride was chosen for its low dielectric loss tangent and high thermal conductivity. The oven core holds the mounted crystals and heaters and acts as the high temperature isothermal enclosure. Its ends are shaped to hold the heaters. The crystals are coated with nichrome and gold then tin soldered to copper electrodes. One crystal is a flat configuration where the electrode comes in from the side as shown in Figure 1. It is mounted between two flat boron nitride pills. The other crystal is placed between two similar electrodes, one above and one below the crystal. It is mounted between two stepped boron nitride pills. The pills are bonded to the electrodes with an RTV cement. The pills are then optically aligned in the oven core and bonded in place using RTV cement. Figure 4 shows an assembled modulator layout in a cutaway view. Figure 5 shows an assembled modulator in an experimental setup. The configuration is typical of all the modulators fabricated during this program except the four crystal modulator, which has the same basic configuration but has a longer oven core to allow the addition of the extra crystal pair and a lens between the crystal pairs.

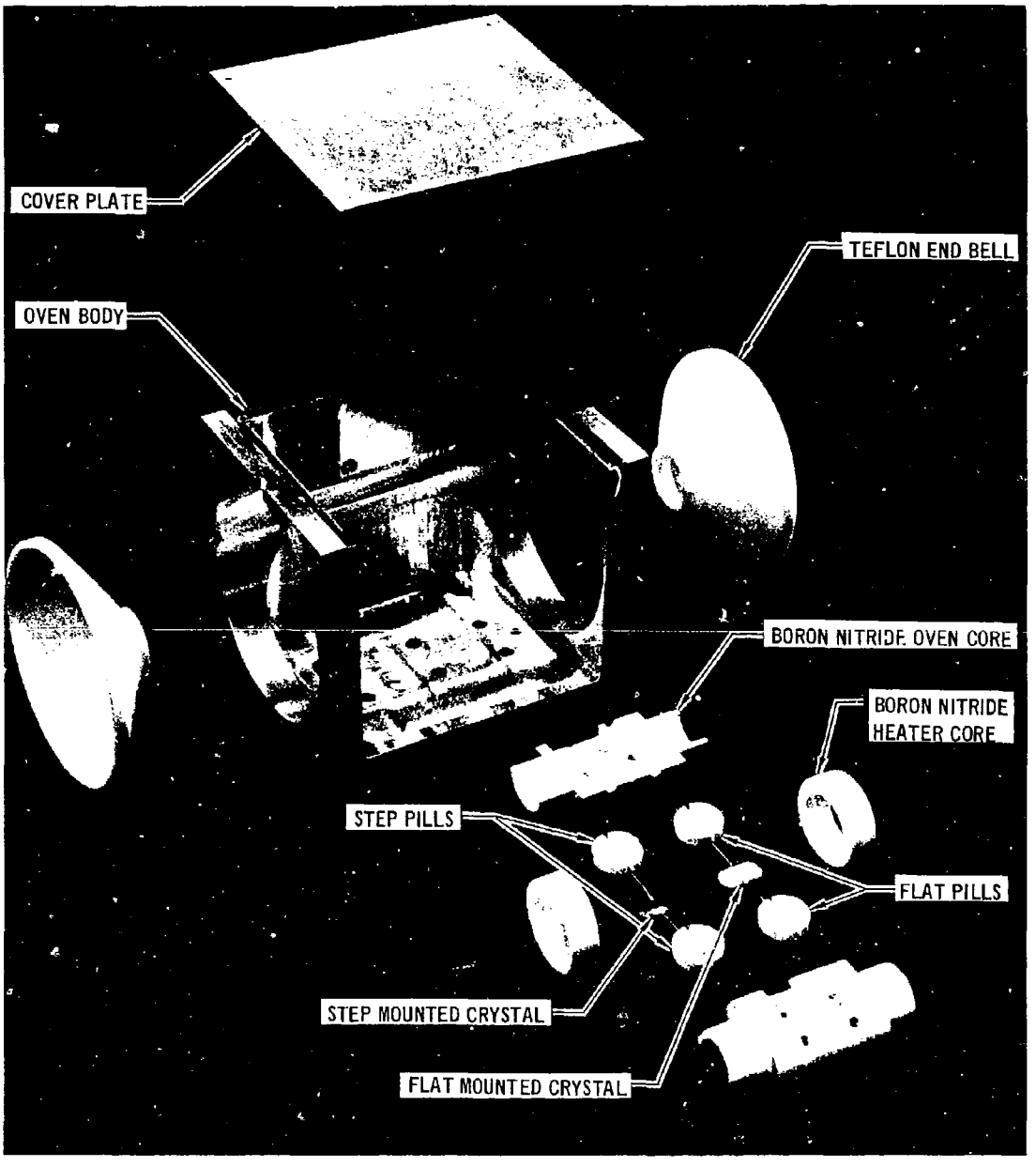

FIGURE 2 OVEN SUBASSEMBLY

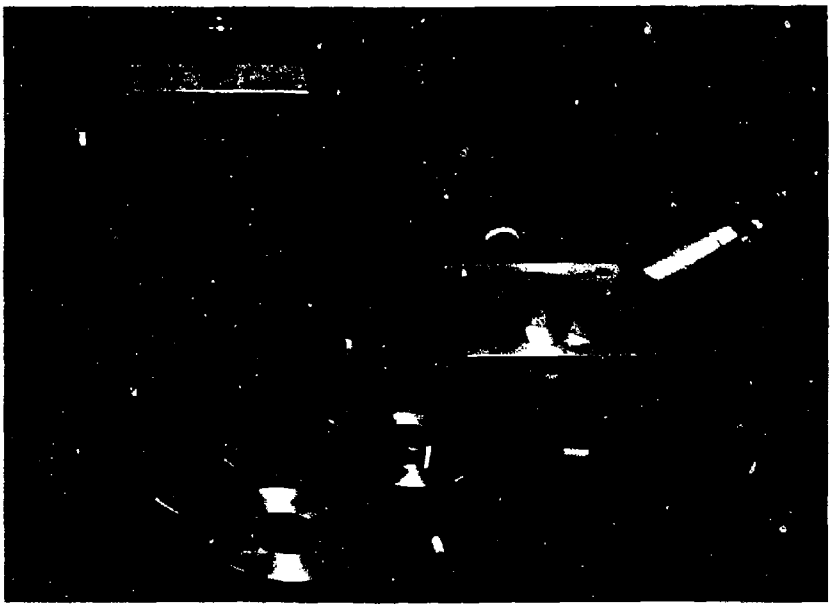

FIGURE 3 FRONT LENS HOLDER

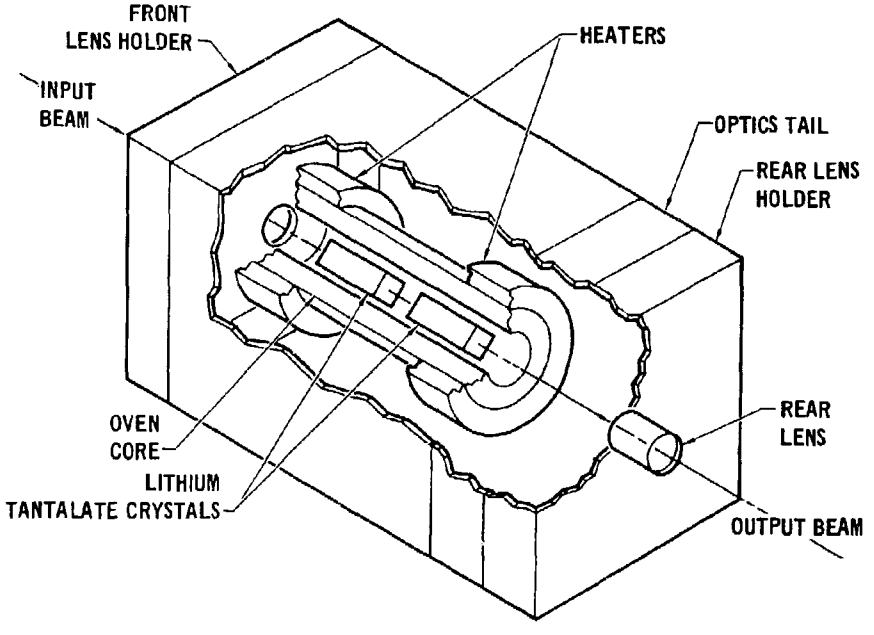

FIGURE 4 MODULATOR SUBASSEMBLY CUTAWAY VIEW

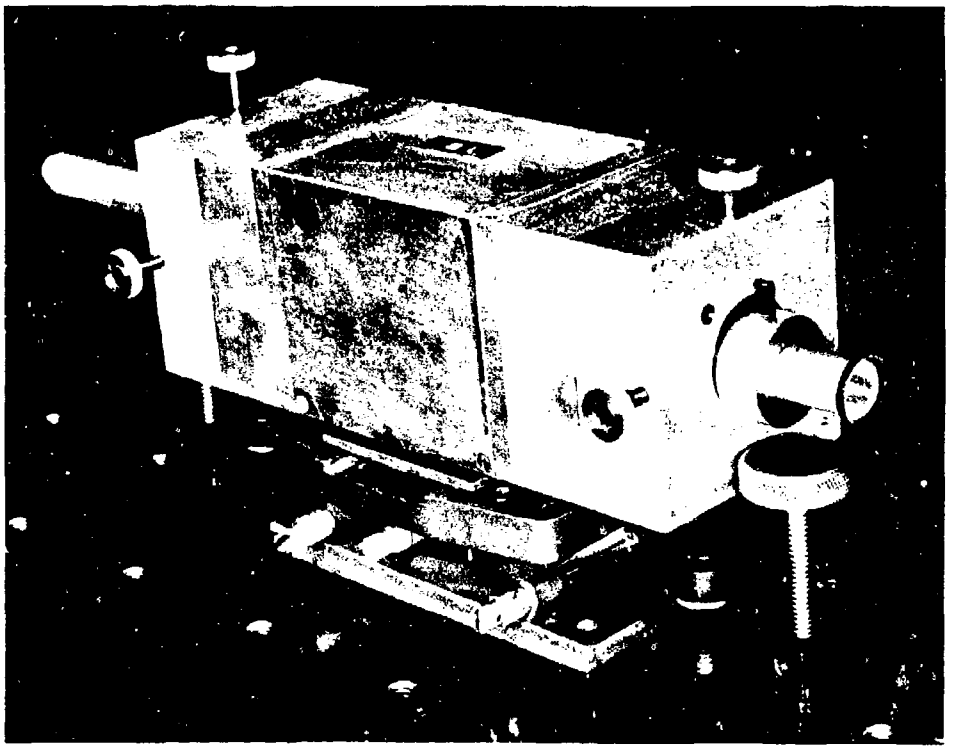

FIGURE 5 PHOTOGRAPH OF ASSEMBLED MODULATOR

We used the same fabrication and crystal mounting techniques that we have used for previous modulators. Residual surface work strain and mounting strain are usually the major reasons for mounted small aperture crystal having a smaller achievable static extinction ratio capability than the large aperture crystal from which they are fabricated. No greater problem was encountered in the fabrication of crystal lengths shorter than 10 mm, or those with a tapered cross section, than was generally encountered in the fabrication of straight 10 mm length crystals. The maximum achievable static extinction ratio of two of the breadboard modulators was less than that of the others due to surface work strain not being removed in the case of the four crystal modulator (AM #2) and mounting strain in the low capacitance modulator (AM #3). In the case of the four crystal modulator, we planned to build a second four crystal modulator with strain relieved crystals if the dynamic switching performance data indicated that that approach was more desirable than the two crystal approaches (which was not the case). The low capacitance modulator was adequate for use in determining if modulator risetime was the limiting factor in modulator performance. The results obtained with both these units (AM #1, AM #3) indicated that little would be gained by fabricating a second of either of these units. We determined instead to use the available time to build a fourth modulator with crystals tapered to reduce switching voltage rather than refine any of the three original design approaches.

2.2 Modulator Design Approach

Figure 6 shows an approximate timing budget for 1 Gbps PGBM. The conditions chosen were laser pulse width 300 ps, electronic timing uncertainty $\pm$ 25 ps, and modulator optical transit time of 75 ps yielding 575 ps available modulator switching time. The optical transit time for 1 cm long crystals was chosen to be 75 ps. For purposes of comparison it was assumed that the 10% to 90% crystal rise time may be added to modulator driver 10% to 90% rise time by root mean square to yield modulator rise time. Actual practice shows this to be approximately the case and that the dynamic extinction ratio worse case bit is primarily determined by the driver output pulse which has the poorest characteristics of risetime and timing accuracy.

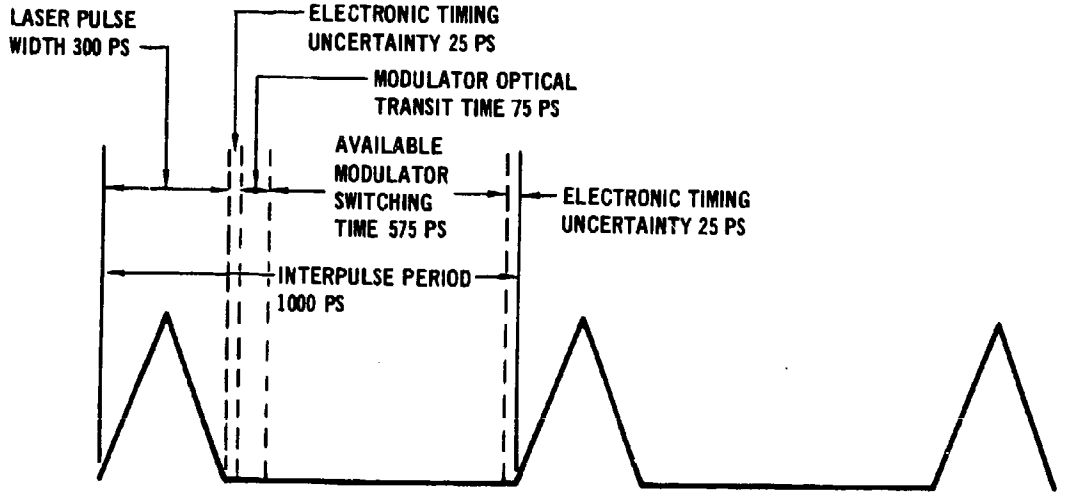

FIGURE 6 TIMING BUDGET FOR 1 ns OPTICAL PULSE SPACING

Figures 7, 8, and 9 show the expected achievable dynamic extinction ratio where the modulator electrical risetime is a linear ramp of the indicated 0 - 100% risetime. Extinction ratio is plotted as a function of driver timing offset from proper timing for laser pulse widths of 300, 400, and 500 ps, and crystal transit time of 75 ps. It is seen that as the laser pulse width increases the required modulator timing accuracy must be increased to achieve the same level of performance. All of the mode locked pulse data were taken with the laser pulse (10% - 10%) adjusted to be less than 400 ps.

The normalized voltage response of a series RC network is shown in Figure 10. It is seen that for 50 ohm impedance and for crystals as small as 5 pf that the normalized voltage response is down several percent for frequencies as low as a few hundred megahertz. The voltage rolloff may be enhanced to second order (as is shown in Figure 11) with better performance at lower frequencies and sharper cutoff at higher frequencies (than the RC network) by the addition of a series inductor whose value is chosen to be $L = R^2C/2$. The modulator optical response of the RC circuit is shown in Figure 12. It is seen that the additional effect of the $\sin^2\tau$ is to hold performance up even more at lower frequencies and produce a sharper cutoff at higher frequencies.

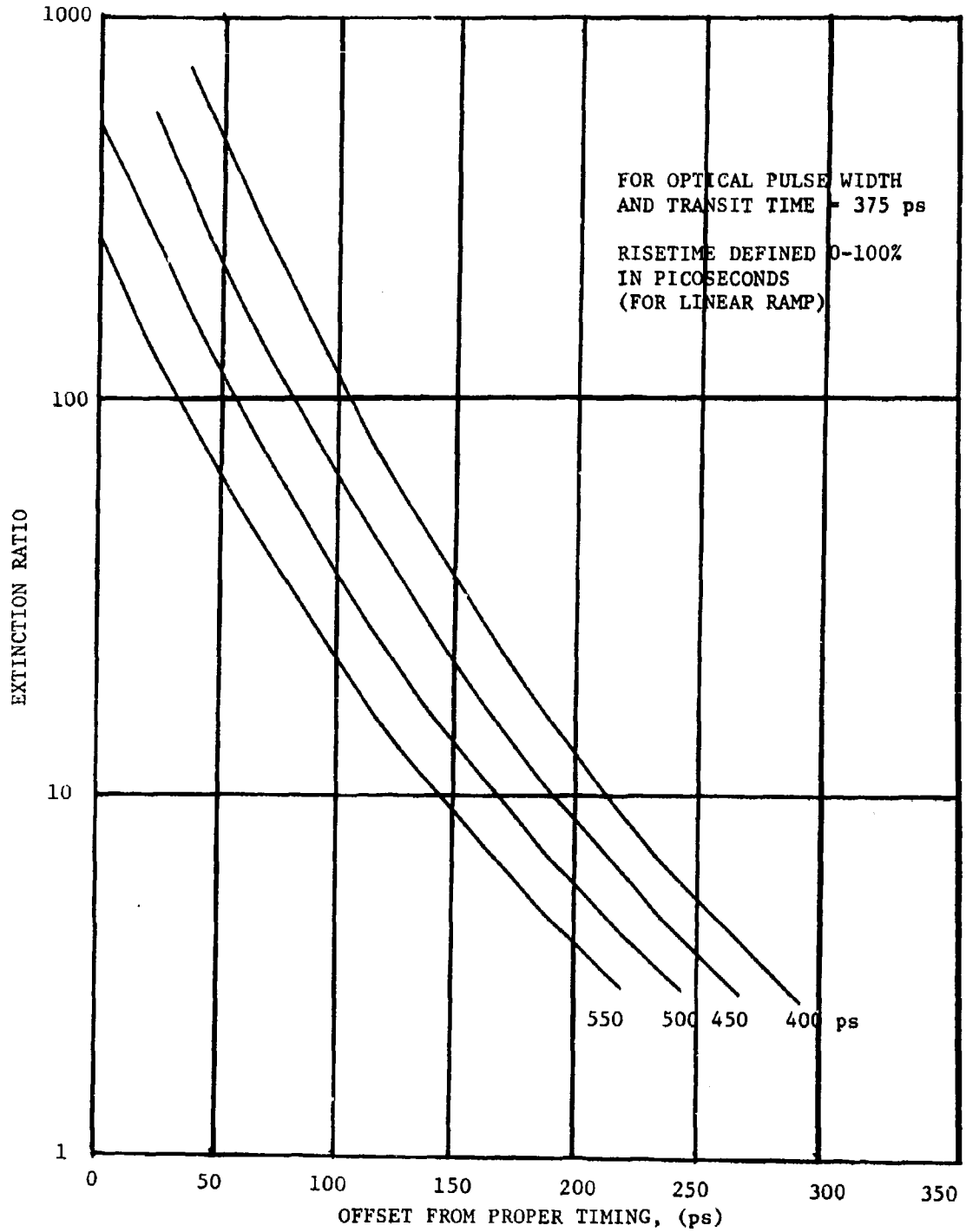

FIGURE 7 EXTINCTION RATIO VS DRIVER TIMING OFFSET FOR AN OPTICAL PULSE WIDTH OF 300 ps

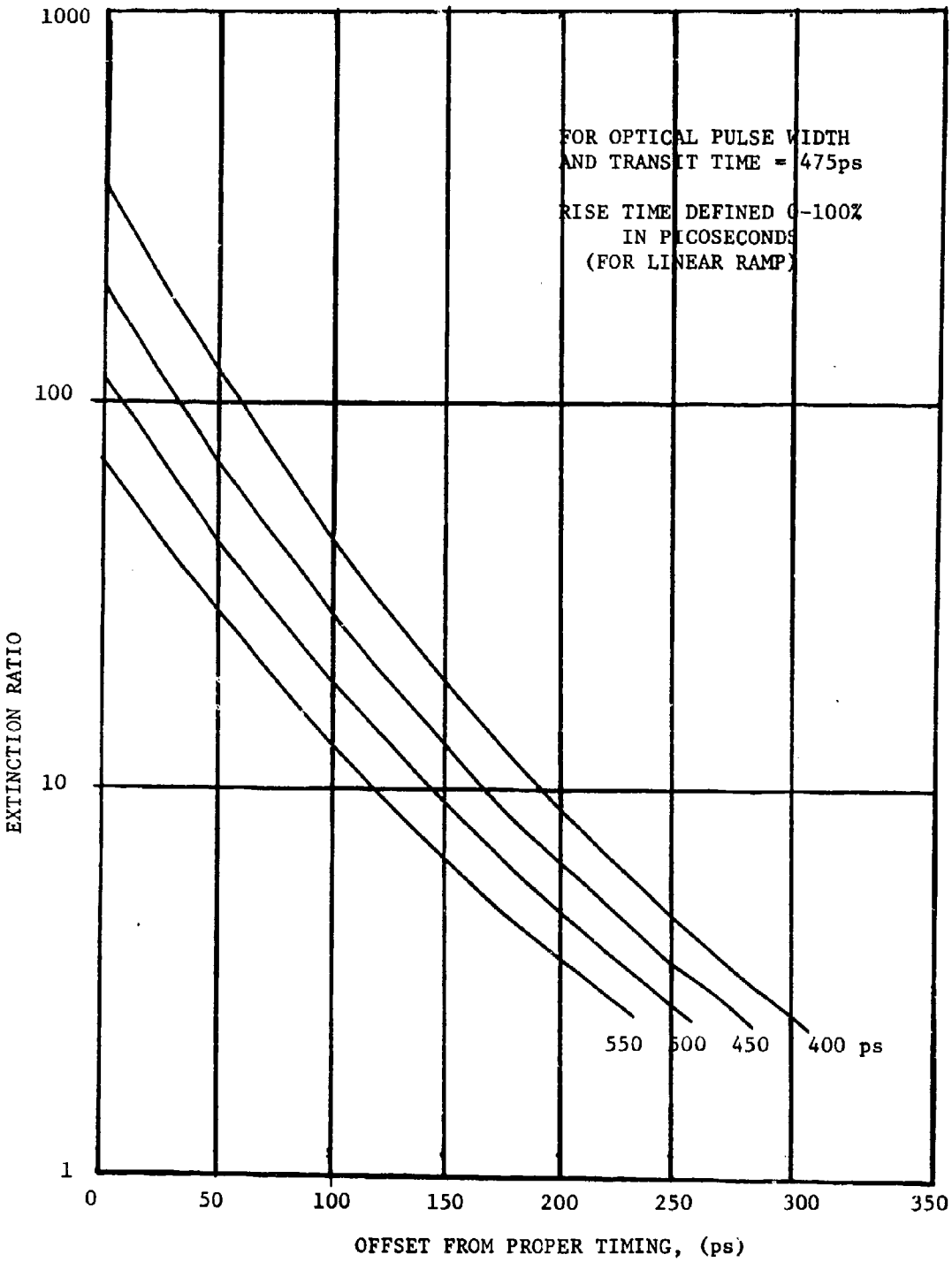

FIGURE 8 EXTINCTION RATIO VS DRIVER TIMING OFFSET FOR AN OPTICAL PULSE WIDTH OF 400 ps

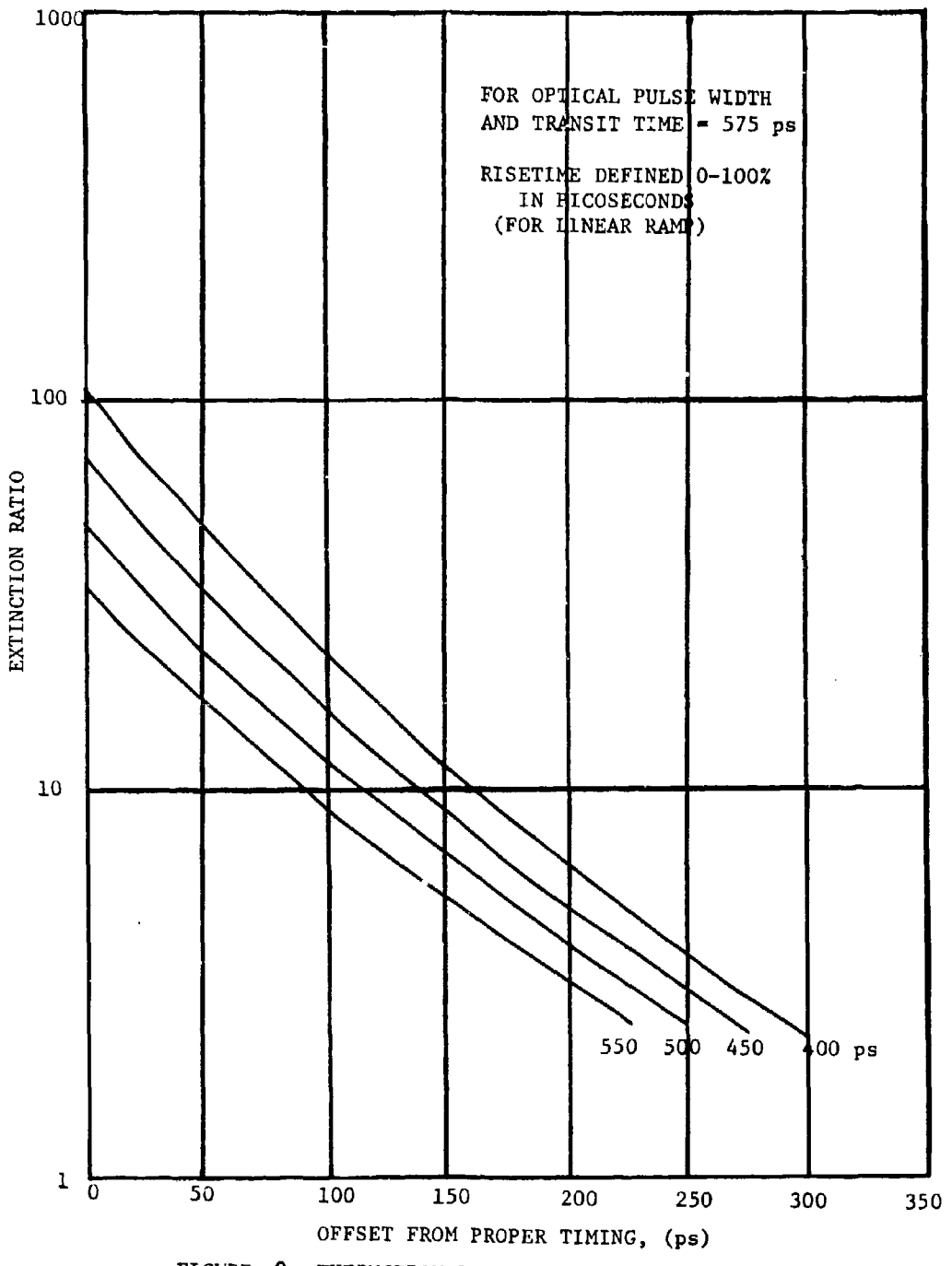

FIGURE 9 EXTINCTION RATIO VS DRIVER TIMING OFFSET FOR AN OPTICAL PULSE WIDTH of 500 ps

The plots of Figures 10, 11, and 12 are informative, but it is difficult to visualize the effect on switching performance when crystal capacitance is changed. One good indicator is to take the energy per unit bandwidth out of the driver and multiply by the crystal responsivity. A resummation of the power will yield a result showing the percent of driver power output actually arriving at the modulator crystal. Figure 13 shows the results of such a calculation using an output spectrum typical of most of our drivers. It is seen that 98% of the driver output power passes to a 3.5 pf crystal (which is typical of the 7 mm length crystals) while no more than 95% of the driver output power passes to a 5.0 pf crystal (corresponding to a 10 mm length crystal). It is to be expected from this analysis that the performance of the lower capacitance crystal would be noticably better than the performance of the higher capacitance, however, actual practice shows that driver timing errors have more effect on performance than do differences in frequency response.

Data similar to that contained in the preceding figures was used to determine several possible crystal size configurations for 1 Gbps operation. At the time the proposal was written, it seemed likely that 100°C operation with lithium tantalate would be possible and was initially chosen as the design temperature to save oven heater power. A list of three possible modulator configurations was given in the proposal. In order to lower switching voltage and improve optical bias stability it was decided that 150°C was a more desirable operating temperature. Table 2 contains the revised list of possible modulator configurations originally selected at the beginning of the program. The first two configurations offered the best performance potential, highest probability of success, and least development. It was determined that the first two configurations would be constructed initially and that the decision as to the configuration of the following units would be based upon the results of the first two units.

$$V_o(f) = [(1-\omega^2 LC)^2 + (\omega CR)^2]^{-1/2}$$

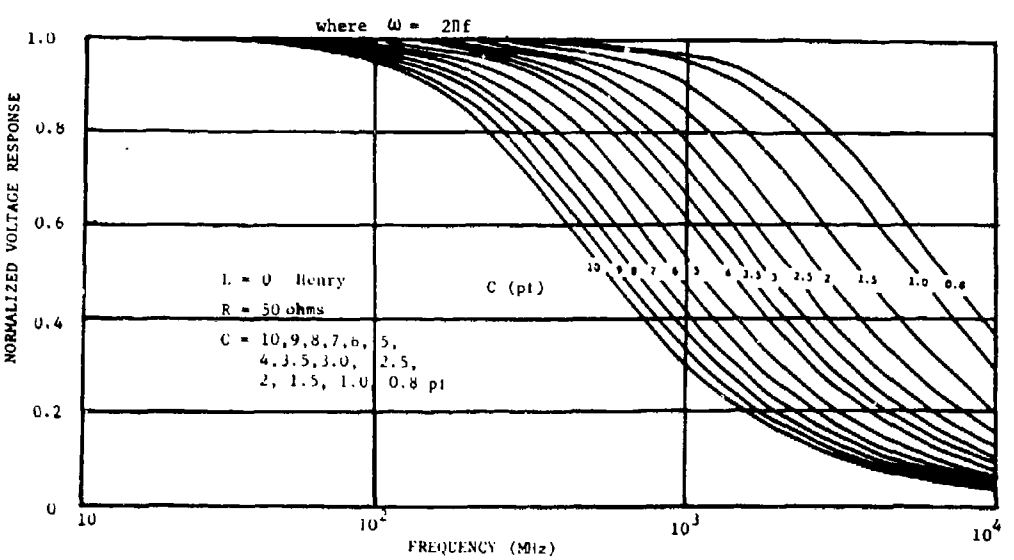

FIGURE 10 MODULATOR RESPONSE WITH A FIRST ORDER MATCH NETWORK

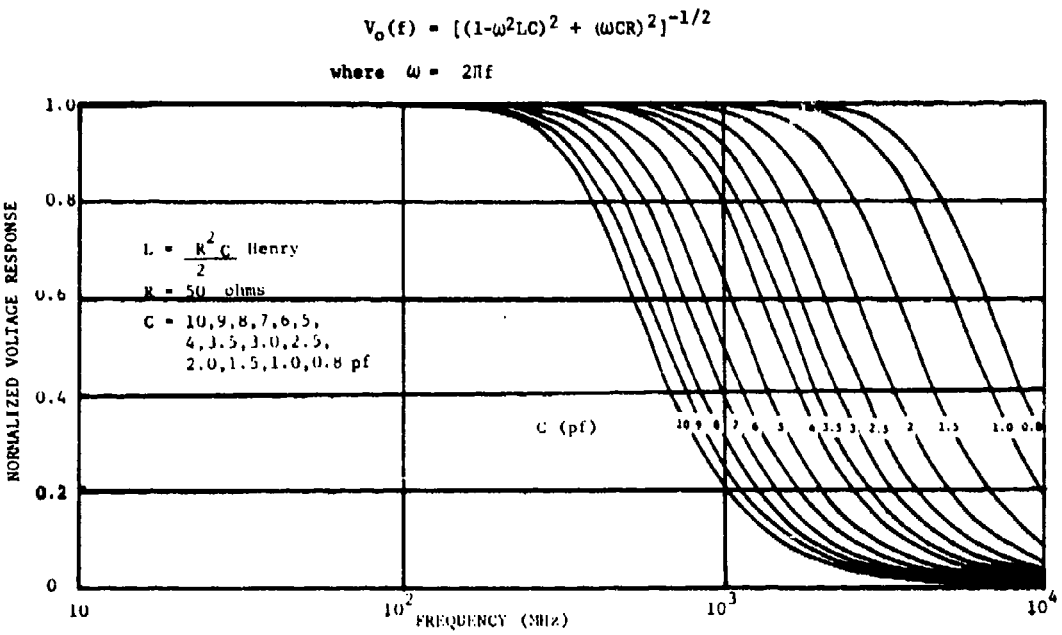

FIGURE 11 MODULATOR RESPONSE WITH A SECOND ORDER MATCH NETWORK

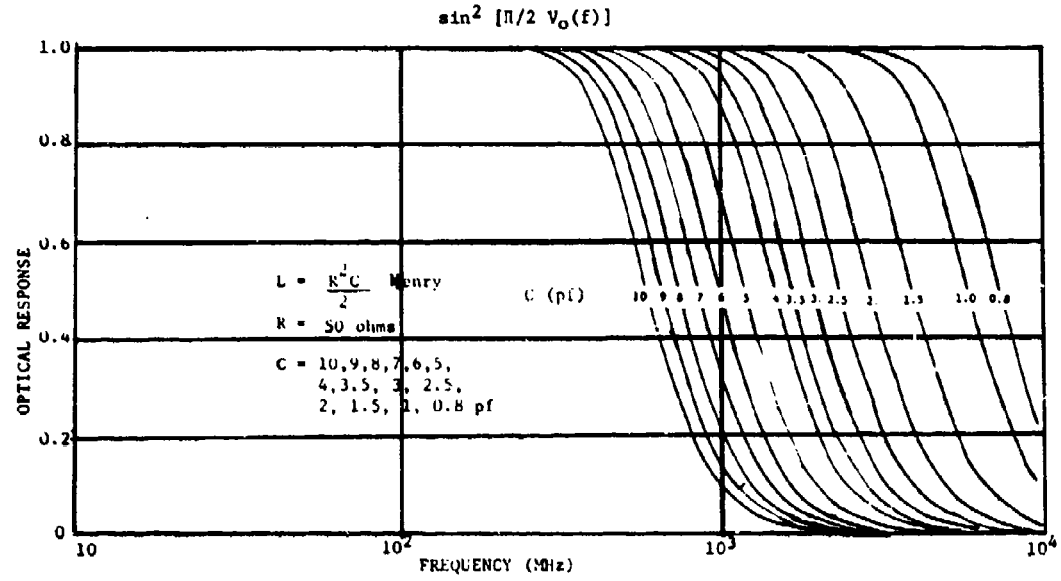

FIGURE 12 MODULATOR OPTICAL RESPONSE FOR SECOND ORDER MATCHING NETWORK

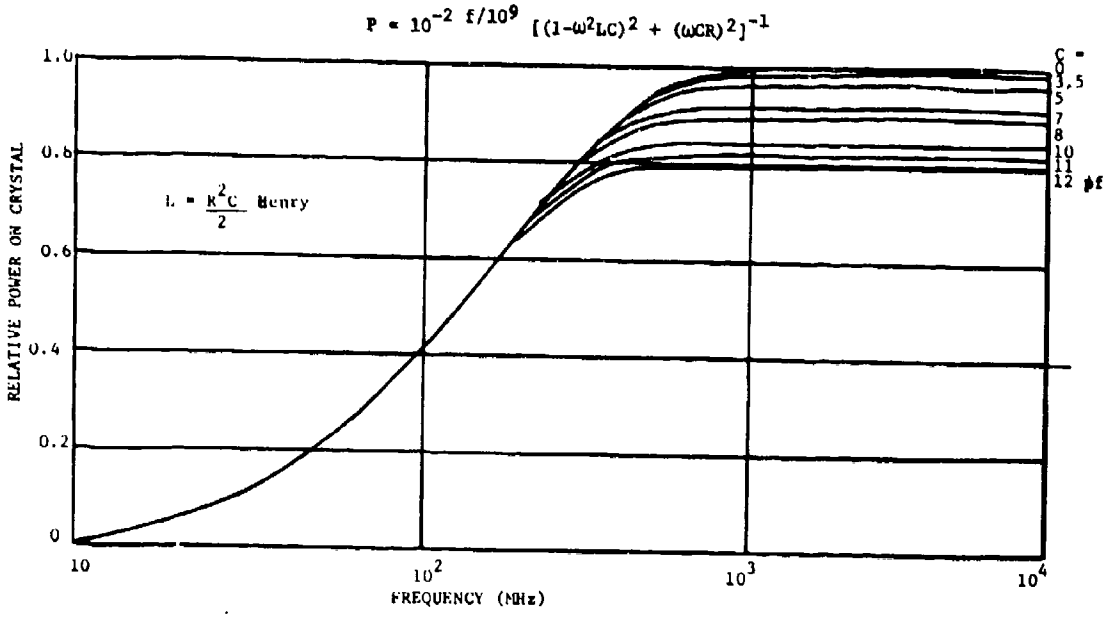

FIGURE 13 RELATIVE CRYSTAL DRIVER POWER FOR SECOND ORDER MATCH NETWORK

TABLE 2. DESIGN PARAMETERS FOR INITIAL MODULATION CONSIDERATIONS

Parameter	Configuration			
	1	2	3	4
Crystal size (mm)	10x0.25x0.25	7x0.25x0.25	15x0.3.0.3	15x0.3x0.3
Number of crystals	2	4	2	2
Crystal temperature (°C)	150°C	150°C	150°C	150°C
Optical transmission	85%	60%	80%	80%
Crystal capacitance (pf)	5/crystal	3.5/crystal	3.75/crystal half	7.5/crystal
Number of parallel inputs (50 ohms)	2	4	4	2 drivers parallel in pairs to 25Ω
Switching voltage (volts)	22	16	20	20
Crystal risetime (ps) (2RC)	500	350	375	375
Driver power in final stage and load (50% duty cycle, watts)	30	35	45	45

The list of modulator configurations actually fabricated is shown in Table 3. Initially AM #1 and AM #2 were fabricated and evaluated. The decision to construct modified versions of 10 mm length crystal modualtors was based upon the finding that the risetime of the two 10 mm crystal modulator with square crystal cross sections, AM #1, was adequate for most bits. The four crystal modulator (AM #2) required much more power than dual input modulators of comparable switching voltage. In addition, we found that the modulator driver timing accuracy improved considerably as the output voltage was decreased. The decreased capacitance modulator (AM #3) showed that a decrease in crystal capacitance alone will not greatly improve modulator performance, while the decreased voltage modulator (AM #4) showed that decreased switching voltage, even with higher capacitance, yielded better performance.

TABLE 3. DESIGN PARAMETERS FOR MODULATOR FABRICATION

	Configuration			
	1	2	3	4
Crystal size (mm)	10x0.25x0.25	7x0.25x0.25	10x0.25x0.25[a]	10x0.25x0.25[b]
Number of crystals	2	4	2	2
Crystal temperature (°C)	150°C	150°C	150°C	150°C
Optical transmission (%)	85%	60%	85%	85%
Crystal capacitance (pf)	5/crystal	3.5/crystal	4.0/crystal	6.25/crystal
Number of parallel input (50 ohms)	2	4	2	2
Switching voltage (volts)	22	16	24	20
Crystal risetime (ps) (2RC)	500	350	400	625
Driver power in final stage and load (50% duty cycle, watt as measured	29.04	40.66	29.04	24.60

(a) B-face tapered from 0.25 mm to 0.15 mm along the 10 mm length.

(b) C-face tapered from 0.25 mm to 0.15 mm along the 10 mm length.

2.3 Modulator Descriptions Including Preliminary Data

As previously mentioned, all our crystalline material except Y3M-268 was GFE from AFAL. This material was evaluated under the Electrooptic Modulator program (F33615-72-C-1989) and the data is given in Technical Report AFAL-TR-72-60. However, as modulator transmission is a problem area in modulator development, further transmission measurements were done on the 3-96 LT lithium tantalate boule. It was found that about 98% of the incident radiation passed through the crystal at Brewster's angle. This indicated surface scattering losses of over 1/2% per surface since internal absorption was much less than 2% as calculated from the absorption coefficient data. When AR

coated, this crystal had transmitted 96% and 96.3% of the incident normal radiation for two different AR coatings. The indication was that the surface finish was inadequate for best transmission when the crystal was AR coated. Transmission greater than 97% had been measured in some of the earlier lithium tantalate, and it was expected that the 3-96 LT material with a better finish would be at least as good as, and probably better than, 97%.

The 50 ohm termination box used with the matching networks was redesigned. It was found that the reflection coefficient in semirigid coax and connector ranged from 2 to 4% at various frequencies. The reflection coefficients in the load box were lowered to less than 4% up to frequencies of 1500 MHz. These loads were satisfactory and did not degrade modulator driver performance.

The approach to the 1 Gbps modulator configuration was identical in crystal configuration to the approach used in the 500 Mbps single-pass modulator brassboard program (AF contract F33615-73-C-1030). Crystals were used in pairs with crossed axes for cancellation of the thermal instabilities and natural birefringence effects. Two modulator configurations were built using two crystal lengths, 7 millimeter and 10 millimeter. The optical safety factor was three. However, one configuration used three variations in crystal cross section since length and the optical safety factor of three was to be conserved in each of the three modulator units. Therefore, four modulators were built as described in Table 3. The modulators were a two 10 mm crystal modulator with square cross section (AM #1), four 7 mm crystal modulator with square cross section (AM #2), two 10 mm crystal modulator with tapered cross section for capacitance reduction (AM #3), and two 10 mm crystal modulator with tapered cross section for voltage reduction (AM #4). Physical descriptions and static performance data will be presented in this chapter and dynamic performance data will be given in chapter 3.

2.3.1 Modulator (AM #1) With Two 10 mm Long Square Cross Section Crystals

The first modulator used two 0.25 mm x 0.25 mm square cross section 10 mm long crystals independently matched to 50 ohms for complementary inputs. The crystals in this modulator unit were fabricated from the 3-54LT-2 boule acquired GFE from contract F33615-72-C-1989. The crystal capacitance was 5.0 pf and required a 24 volt driver for full half-wave switching at 150°C. The required driver power was 30 watts. The voltage reflection coefficient was less than 4% up to 1.0 GHz for each of the crystals. This 4% reflection was approximately equal to a VSWR value of 1.08. The static transmission was 80% for this modulator and it had a static extinction ratio of 17 dB. Figure 14 shows the static extinction ratio for this modulator. Both the

STATIC
EXTINCTION RATIO: 17 dB

ON — 20 dB Attenuation

OFF — 0 dB Attenuation

FIGURE 14 STATIC EXTINCTION RATIO OF A TWO 10mm LONG CRYSTAL 24V MODULATOR (AM #1)

transmission and static extinction ratio limitations were due to the quality of the particular crystalline material from which the crystals were cut and were not indicative of the performance obtainable with the best quality lithium tantalate material. This performance level was satisfactory for breadboard modulator applications to evaluate dynamic performance.

2.3.2 Modulator (AM #2) With Four 7 mm Long Square Cross Section Crystals

The second modulator used two pairs of two 0.25 mm x 0.25 mm cross section 7 mm long crystals in series optically in a single oven. Each crystal was matched to 50 ohms with each crystal pair being driven by complementary driver inputs. This modulator was fabricated using 3-90LT - 7 mm long crystal material acquired GFE from contract F33615-72-C-1989. The crystal capacitance was 3.5 pf and required 17 volt half-wave switching voltage at 150°C. The required driver power was 35 watts. The voltage reflection coefficient was less than 8% up to a frequency of 1.5 GHz at 150°C. This 8% reflection was approximately equal to a VSWR value of 1.18. Optical alignment of this modulator was more difficult than for the AM #1 unit as there were four crystals arranged in crossed axis crystal pairs with a lens between the crystal pairs. Thus this approach was less efficient optically than AM #1 because of the extra crystal surfaces and lens. The static transmission of this modulator was measured to be only 40%. The achievable static extinction ratio was not quite as high as with two crystal modulator units because of the longer optical path in the lithium tantalate material. The static extinction ratio was only 11 dB for this four crystal modulator unit, however this was adequate to evaluate modulator switching performance. Two drivers were used with this modulator unit, one for each crystal pair; each driver had complementary outputs. It was believed that due to the reduced switching voltage and improved pulse rise times that the dynamic performance would be very good. However, even with the reduced half-wave switching voltage (17 volts) the total required driver power was considerably higher (~15%) than that of the two 10 mm long crystal modulator (AM #1) approach.

2.3.3 Modulator (AM #3) With Two 10 mm Crystals Tapered for Capacitance Reduction

This modulator was a modified version of the two crystal 0.25 mm x 0.25 mm square cross section 10 mm long lithium tantalate modulator and takes advantage of the fact that the optical beam was about 70 μm smaller in diameter at the center of the modulator than at the ends. With a safety factor of three the beam diameter is 234 μm at the faces and 165 μm in the center of the modulator. This modulator used a tapered pair of crystals which had the b-faces ground off to give a thickness of 0.15 mm at one end while maintaining a thickness of 0.25 mm at the other end. Figure 15 illustrates the tapered crystal configuration and gives the dimensions and crystal axis. The small crystal ends were at the center of the modulator unit where the laser beam was more tightly focused. This crystal tapered in the b-faces does not affect the switching voltage, since the thickness was kept 0.25 mm in the c-axis, but does decrease the capacitance by one picofarad (twenty percent) compared to the 0.25 mm square cross section 10 mm long crystal. The net result due to the lower crystal capacitance was that the modulator should have the same optical transmission as the two-crystal modulator previously described, but should have twenty percent faster rise time capacility. This twenty percent improvement in rise time was expected

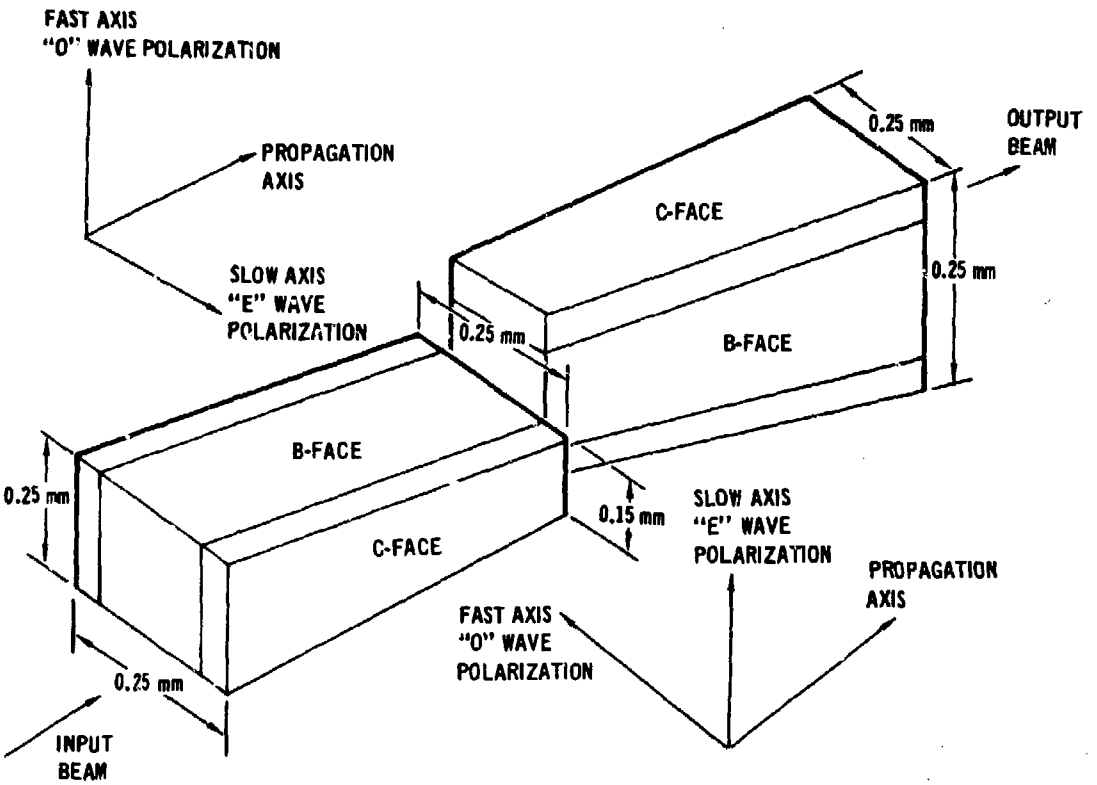

FIGURE 15 CRYSTAL MOUNTING ARRANGEMENT FOR CRYSTAL MODULATOR TAPERED FOR CAPACITANCE REDUCTION

to yield significantly better performance with the existing drivers at that time. However, the performance was not significantly improved indicating driver timing accuracy as being perhaps the most critical parameter of the driver for optimum modulator performance at this present state-of-the-art driver development. This modulator was fabricated using 3-96LT 10 mm long crystal material obtained GFE from the crystal development program (F33615-72-C-1989). The crystals were individually matched to 50 ohms. The crystal capacitance was 4.0 pf and required 24V driver for full half-wave switching at 150°C.

The required driver power was 30 watts. Each modulator crystal had voltage reflection coefficient less than 8% up to a frequency of 1.5 GHz at 150°C. The optical transmission for this modulator was 77%. There was mounting strain in the crystals of this modulator which limited the static extinction ratio of 14 dB. The optical safety factor for this modulator was the same as for the square crystal modulator, which was three. The alignment of the crystals in the modulator presented very little increased problem over alignment of the square crystals. It was found, however, that the incoming beam divergence must be 20% nearer confocal focusing for best operation than with the square crystal modulator.

2.3.4 Modulator (AM #4) With Two 10 mm Crystals Tapered for Switching Voltage Reduction

In order to lower the switching voltage requirement of the modulator drivers, it was decided to taper the modulator crystals for decreased switching voltage so that a 20 volt modulator with better dynamic switching performance could be obtained. Therefore, a unit with crystals tapered for decreased switching voltage was built for 20 volt operation, without decreasing the crystal optical safety factor or limiting the static transmission or extinction ratio. The modulator fabricated had two 10 mm long crystals tapered for reduced switching voltage with the cross section of 0.25 x 0.25 mm at the large end and tapered to 0.25 x 0.15 mm at the small end with the taper occurring between the sides attached to the electrodes (c-faces). Therefore, this modulator used a pair of tapered crystals which had their c-faces ground off to give a thickness of 0.15 mm at one end while maintaining a thickness of 0.25 mm at the other end, see Figure 16. When assembled into the modulator the crystals were oriented so that the small ends were at the modulator center in order to maintain an optical safety factor of 3 for beam alignment purposes. The crystal tapered in the c-faces as described reduced the switching voltage by 20%; however, the capacitance was increased by 25%. Therefore, it was decided to investigate the optical response of a tapered c-face modulator crystals to check the crystal rise time for potential problems. Figure 17 shows the optical response to a 500 MHz PN code generator non-return-to-zero (NRX) data input. The optical response appeared to be well within 100 ps of the NRZ data input. Figure 18 shows the optical response to 1 GHz NRZ data input.

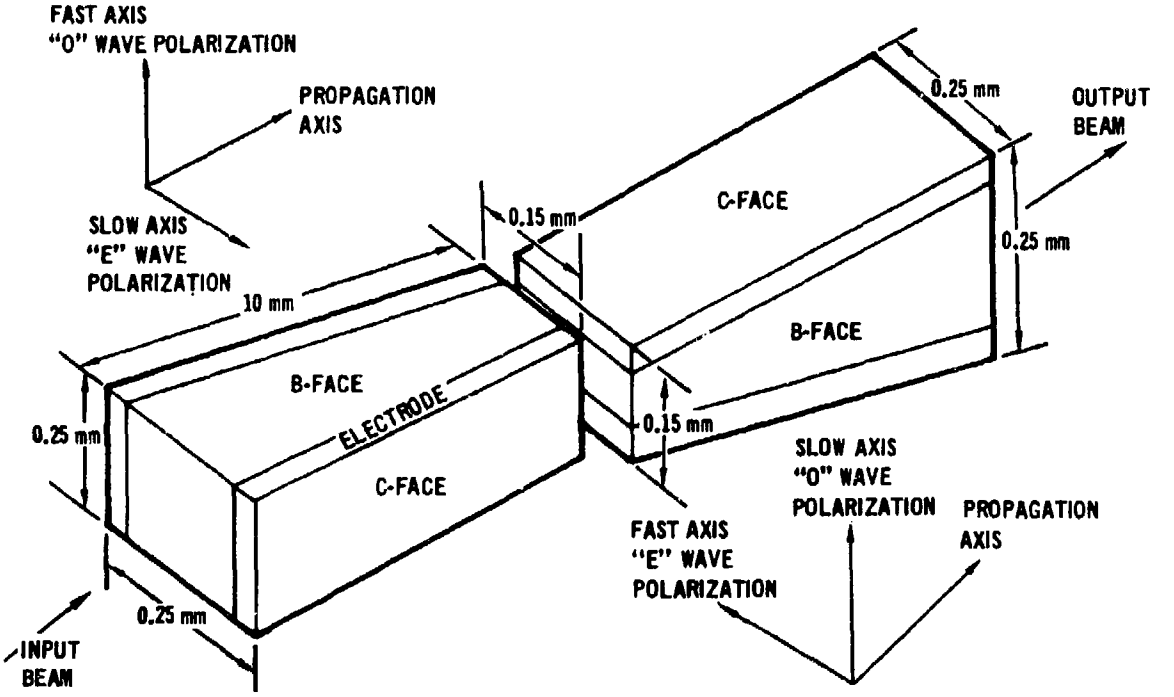

FIGURE 16 CRYSTAL MOUNTING ARRANGEMENT FOR CRYSTAL MODULATOR TAPERED FOR SWITCHING VOLTAGE REDUCTION

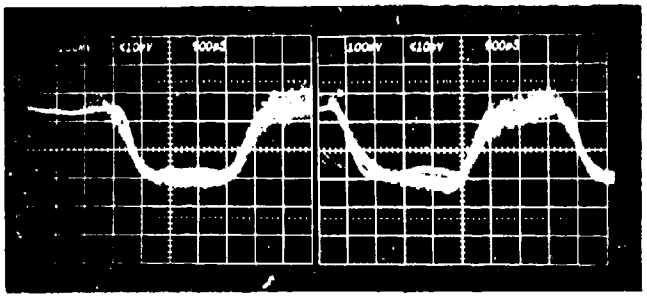

FIGURE 17 OPTICAL RESPONSE OF A SINGLE CRYSTAL TAPERED FOR VOLTAGE REDUCTION IN RESPONSE TO 500 Mbps NRZ DATA

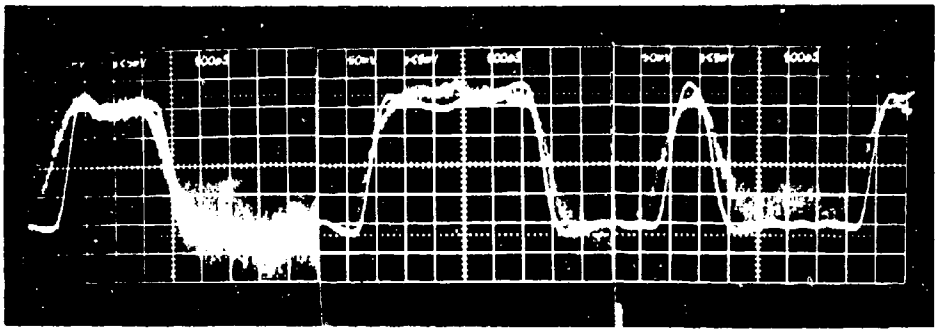

FIGURE 18 OPTICAL RESPONSE OF A SINGLE CRYSTAL TAPERED FOR VOLTAGE REDUCTION IN RESPONSE TO 1 Gbps NRZ DATA

The crystal response was not as fast, however, it was less than 200 ps. This data was acquired using a 24 volt driver (SSD #4) which was not adequate for full half-wave switching (required 38 volts) of the single crystal. The laser used was a CW krypton with the output wavelength of 0.53 μm.

This two crystal tapered c-face modulator was fabricated from crystalline material, Y3M268, obtained from Crystal Technology Inc. by MDAC. This modulator had crystals individually matched to 50 ohms. The crystal capacitance was 6.25 pf and required 20V driver for full half-wave switching at 150°C. The required driver power was 25 watts. Each modulator crystal had voltage reflection coefficient less than 8% up to a frequency of 1.5 GHz at 150°C. Optical transmission measurements were performed for the voltage tapered modulator and a transmission value of 81.5% was obtained. This value was comparable to the results obtained for the brassboard modulators (85.3%) in the Laser Modulator II program (F33615-73-C-1038), and was within the goal set for this program. The static extinction ratio measured 90:1 for this voltage tapered modulator. The dc switching voltage required to produce full half-wave switching was 19.8 volts. This was a decrease of approximately 4 volts, or 20%, from the values obtained for 0.25 mm x 0.25 mm straight crystal modulator (AM #1) not utilizing crystals tapered to reduce switching voltage.

2.4 Modulator Drivers

Existing 500 Mbps Modulator driver circuit configurations were used as the starting point for the 1 Gbps program. Figure 19 is a block diagram of the modulator driver. A single ended input signal drove an emitter coupled pair (ECP) as the first stage. This emitter coupled pair drove a second emitter coupled pair double ended. The second emitter coupled pair drove a third emitter couple pair double ended. Two complementary outputs from the third emitter coupled pair were buffered and each routed through two gain stages to develop the required output levels.

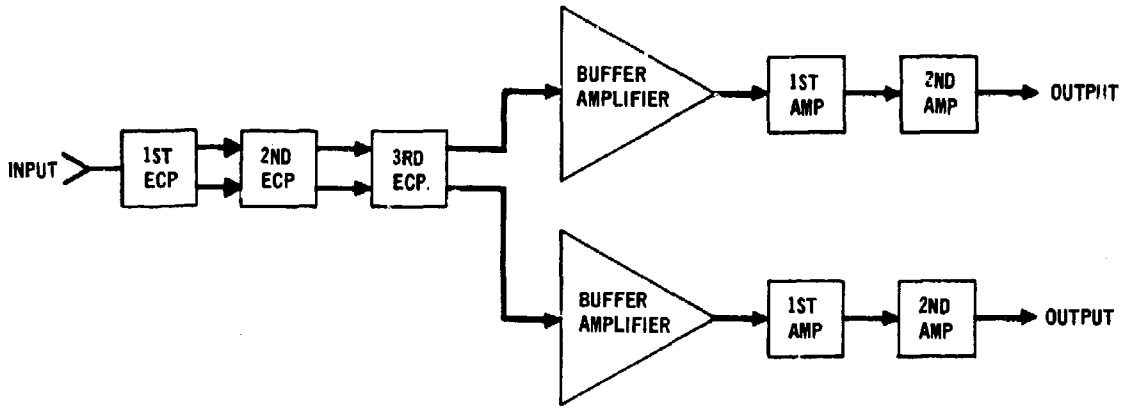

FIGURE 19 MODULATOR DRIVER AMPLIFIER

The first step in the driver portion of this effort was to upgrade the performance of a single output driver so that it would be able to make the required voltage transitions at a 1 Gbps rate. The next step was to build a similar unit having the required additional components to deliver two complementary output waveforms at a 1 Gbps rate. Initially the output voltage swings of the dual output driver (SSD #1) were 20 volts peak-to-peak but the timing accuracy of transitions of the output voltage differed by as much as 400 ps from the proper time of occurrence, as determined by comparison with the actual input waveform to the driver. Timing fidelity was difficult to maintain in discrete component modulator drivers because uncontrollable parasitics added overshoot and some ringing to the circuits. This problem of unavoidable and irreproducible parasitics was minimized in thin film hybrid circuits. Therefore, the second version of 1 Gbps dual output driver used thin film hybrid circuits to accomplish a major portion of the total required amplification in the front stages of the driver from 0.5 volts to 5 volts. Two such units were built each having 17 to 18 volts complementary outputs. Timing deviations were on the order of $\leq \pm$ 200 ps in these units. These units were numbered SN MD2-002 and SN MD2-003.

Since higher output voltages were required for some modulators, the gain of the output stages on the dual output discrete component modulator driver (SSD #4) was increased to yield 24 volt transitions. Timing inaccuracies measured $\leq \pm$ 350 ps. This modified driver will be denoted SSD #4 in the text.

In order to supply 20 volt drive signals having timing inaccuracies as small as possible, the output stage gain of one of the hybrid preamp modulator drivers (SNMD2-002) was boosted to deliver 20 volt peak-to-peak swings. The timing inaccuracy of this driver's outputs were less than $\pm$ 200 ps with respect to the system clock when using a signal source having $\pm$ 70 ps timing inaccuracy, but there was one particular isolated pulse in the code which had its rise occur late and its fall occur early. This modified driver will be denoted as SSD #5 in the text. This prompted us to build another discrete component modulator driver (3X) with two complete parallel chains of small signal input stages. This discrete component modulator driver was built consisting of 2 parallel chains of emitter coupled pairs which drove 2 higher current stages having 20 volt output swings. This driver was similar in design to the hybrid circuit and discrete component drivers previously described, but had two extra low power stages added so that lower gain per stage was used which produced better overall timing accuracy. This unit exhibited 20 volt swings with $\leq \pm$ 175 ps timing inaccuracies with respect to the system clock using a signal source with $\leq \pm$ 70 ps of timing inaccuracy. This drivers output did not have individual pulses which were both as late rising and as early falling as the previously mentioned hybrid driver.

The power spectrum of a 1 Gbps driver (SSD #1) was measured and it was determined that it falls off at about 20 dB/GHz. Figure 20 shows the driver output response. When the driver output was multiplied by the matching network response of the above mentioned 7 mm and 10 mm crystals, it was found that 98% of the driver power passes to the 7 mm crystal and 95% of the driver power passes to the 10 mm crystal, as seen in Figure 13. It was noted that these numbers do not indicate the bit by bit performance of the 7 mm and 10 mm crystal, but they did indicate that the switching performance of the 10 mm crystals would be noticeably poorer than that of the 7 mm crystals.

The effect of modulator driver timing error on the dynamic extinction ratio for 1 Gbps operation was calculated and is shown in Figures 7, 8, and 9. The only difference in these figures were the allowable laser pulse width, which was 300, 400, and 500 ps respectively. The modulator crystal transit time was 75 ps. The modulator rise was assumed to be a linear ramp. It was seen in the figures that little timing error was allowable for rise times over 500 ps and that as the modulator rise time was decreased, there was a corresponding increase in allowable timing error. During this program we went from 400 ps timing error to our present level of 175 ps timing error on some gates. The drivers using a thin film hybrid circuit for the amplifiers up to the 5 volt level originally had 100 ps less timing error than did our discrete component drivers but they also had only 18 volts maximum output. However, the last discrete component driver with 20 volts $\pm$ 1 volt output had less timing error ($\leq$ 25 ps) than the thin film hybrid circuit front stage drivers. The dynamic performance test results show how critical driver timing accuracy is for optimum modulator performance, and to reiterate the need for good driver timing accuracy can be seen in Figure 7, 8, and 9.

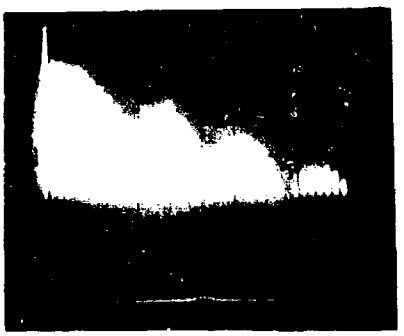

(a) Repetition Code Timing
2ns Pulse with 20ns Spacing

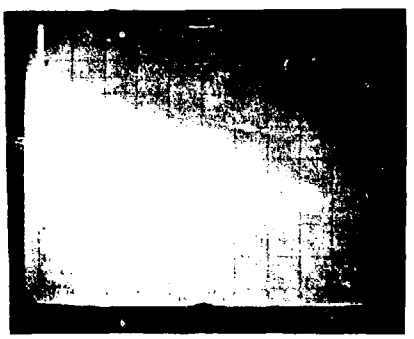

(b) Repetitive Code Input
2ns Pulse with 50ns spacing

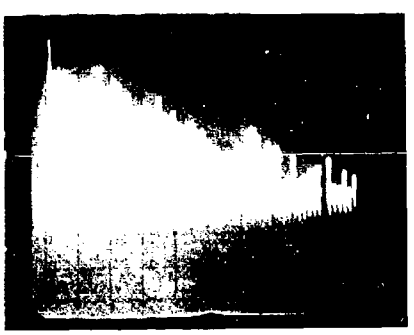

(c) 1 Gbps PN Code Input
Best Driver Adjustment

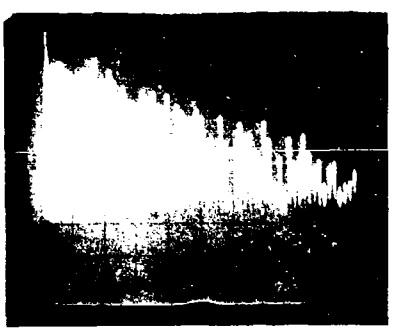

(d) 1 Gbps PN Code Input
Poor Driver Adjustment

FIGURE 20 DRIVER SPECTRAL OUTPUT
Horizontal 0 to 2 GHz full width
Vertical is 10 dB/div

3. PERFORMANCE TESTS

During this program four different modulator configurations were evaluated in a test bed for 1 Gbps PGBM performance. The modulators vary in the number of crystals per unit, length of crystals, crystal cross section, crystal boule, crystal capacitance, and switching voltage. The static optical transmission (crystals only), static extinction ratio, dc half-wave switching voltage, dynamic extinction ratio and voltage reflection coefficient were measured for each advanced modulator unit. Table 4 lists performance characteristics of the solid state modulator drivers which were used in these modulator/modulator driver evaluations. Table 5 summarizes the static parameters for the four $LiTaO_3$ 1 Gbps modulators and their static performance.

The optical transmission, which was measured in all cases for the modulator crystals only, was approximately 80% for all three of the two 10 mm crystal modulators. The addition of another pair of crystals and a lens between the two pair lower the static transmission in the four 7 mm crystal modulator (AM #2). When the work stain and mounting stain was removed from the modulator crystals a static extinction ratio better than 50:1 was obtained and with the proper modulator driver a dynamic extinction ratio greater than 17.5:1 was obtained. The modulator matching network was always less than 8% up to frequencies of 1.5 GHz for each crystal.

The laser used for these evaluations was the 500 Mpps breadboard mode-locked and frequeny doubled Nd:YAG laser. The laser pulsewidth for these evaluations ranged from 300 to 350 ps at the 10 - 10% points. The linear polarized laser output was changed to circular polarization by passing the beam through a Senarmont Compensator. The beam which is then a composite of s-wave and p-wave (polarizations) is then split by a polarization splitter, the s-wave passes straight through the polarization splitter cube and the p-wave is reflected 90° from the s-wave. The p-wave is then sent through a 1 nanosecond time delay optical path (30 cm) and then recollimated with the s-wave at a polarizer combiner cube as seen in Figure 21. This is how the 500 Mpps laser was multiplexed to a 1 Gbps optical wave train. The optical detector was a T1XL55 silicon avalanche photo diode which was marginally adequate for evaluation of the 1 Gbps modulator. This same photo diode was used in obtaining all the modulator data with all four modulator units.

3.1 Modulator (AM #1) With Two 10 mm Long Straight Crystals

Figure 22 shows the dynamic performance of this modulator. The driver used for these evaluations was a driver developed for use with the 7 mm crystal (MD-2-003) modulator therefore it had only 18 volts dynamic switching capability. Since the driver was under the halfwave switching voltage the data was poor; in fact, the worst case dynamic extinction ratio was $\geq$ 7:1.

This same modulator also had been operated with an entirely discrete component driver (SSD #4) which provided full switching voltage, but did not have good timing symmetry. The timing inaccuracies were $\leq \pm$ 350 ps. The worst case dynamic extinction ratio was about 8:1 for the transmitted and the rejected polarizations. Figure 23 shows the driver waveforms and the detected optical 1 Gbps PGBM data. Improved driver performance would improve the dynamic

TABLE 4. SUMMARY OF SOLID STATE DRIVER PERFORMANCE

Driver Number	Output Voltage (p-p)	Timing Inaccuracy	Rise/Fall Time	Power Required	Type of Circuit
SSD #1	20 volt	$\leq \pm$ 400 ps[d]	400 ps min 500 ps max	26.07 watts	Discrete component
MD-2-002	17 volt	$\leq \pm$ 200 ps[e]	400 ps min 500 ps max	20.03 watts	Front stage thin film hybrid, output stage discrete component
MD-2-003	18 volt	$\leq \pm$ 200 ps[e]	400 ps min 500 ps max	20.63 watts	Front stage thin film hybrid, output stage discrete component
SSD #4	24 volt	$\leq \pm$ 350 ps[d]	400 ps min 500 ps max	29.04 watts	Discrete component (a)
SSD #5	20 volt	$\leq \pm$ 200 ps[e]	400 ps min 500 ps max	23.63 watts	Front stage thin film hybrid, output stage discrete component (b)
3X	20 volt $\pm$ 1 volt	$\leq \pm$ 175 ps[e]	400 ps min 500 ps max	24.60 watts	Discrete component (c)

Notes: (a) SSD was modified by increasing the gain stages; SSD #4 is the modified unit.

(b) MD-2-002 was modified by increasing the gain stages; SSD #5 is the modified unit.

(c) 3X differs from the other discrete component drivers in that it amplifies through two complete parallel chains of small signal input stages.

(d) Timing inaccuracies measured relative to input signal.

(e) Timing inaccuracies measured relative to system clock.

TABLE 5. STATIC PARAMETERS FOR $LiTaO_3$ 1 Gbps MODULATOR

Modulator Number	Number of Crystals	Crystal Size			Boule Section	Capacitance	Optical Safety Factor	Static Optical Transmission	Static Extinction Ratio
		length a-axis	cross section b-axis	c-axis					
AM #1	2	10 mm	0.25 mm	0.25 mm	3-54LT-2	5 pf	3	80%	50:1
AM #2	4	7 mm	0.25 mm	0.25 mm	3-90LT-7	3.5 pf	3	40%	12:1
AM #3	2	10 mm	0.25 mm tapered to 0.15 mm	0.25 mm	3-96LT	4.0 pf	3	77%	25:1
AM #4	2	10 mm	0.25 mm	0.25 mm tapered to 0.15 mm	Y3M268	6.25 pf	3	81.5%	90:1

Each crystal was impedance matched to 50 ohms at 150°C. Each modulator unit was operated at 150°C.

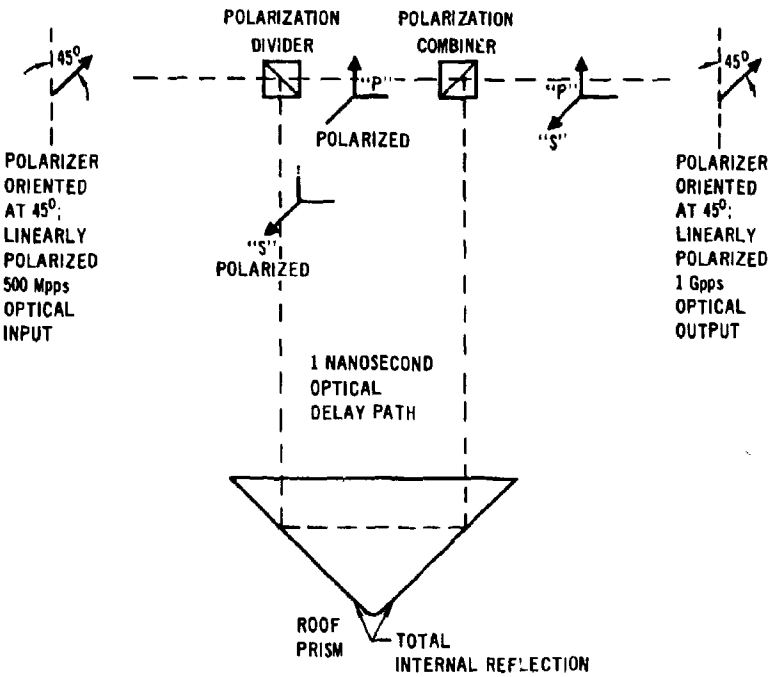

The linearly polarized optical input is a 500 mpps optical wave train composed of two orthogonal polarizations of equal amplitude which are separated by the polarization divider. The "p" polarization goes on to the polarization combiner, the "s" polarization is delayed by one nanosecond before it reaches the polarization combiner. At the polarization combiner the two polarizations are combined(with the "s" polarization pulses delayed one nanosecond with respect to the "p" polarization pulses). This combined beam is then linearly polarized by a polarizer at 45° resulting in a 1 Gpps optical wave train.

FIGURE 21 TIME DELAY UNIT FOR MULTIPLEXING 500 Mpps OPTICAL INPUT TO 1 Gpps OPTICAL OUTPUT

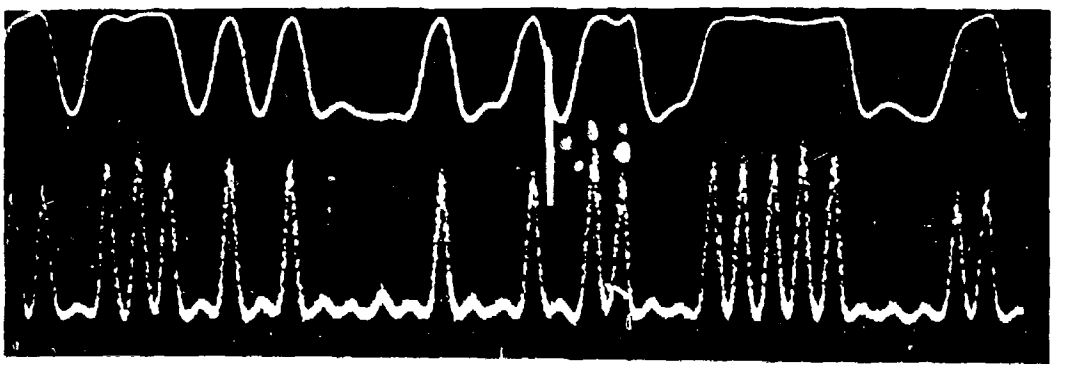

The upper trace is the Modulator Driver Waveform Vertical Scale 10 volts/div; Horizontal Scale 2 nsec/div.
The lower trace is the Modulated optical Signal - Worst Case Extinction Ratio $\geq$ 7:1

FIGURE 22 1 Gbps PGBM DATA TAKEN USING THE 24 VOLT MODULATOR (AM #1) WITH THE 18 VOLT DRIVER (MD-2-003)

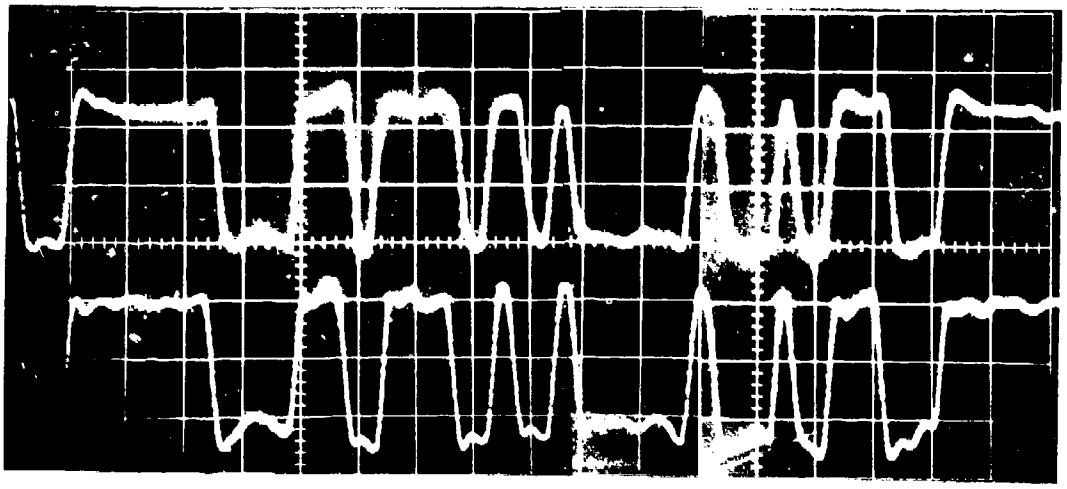

(a) Modulator Driver Output
Vertical Scale 10 volts/div; Horizontal scale 2 nsec/div

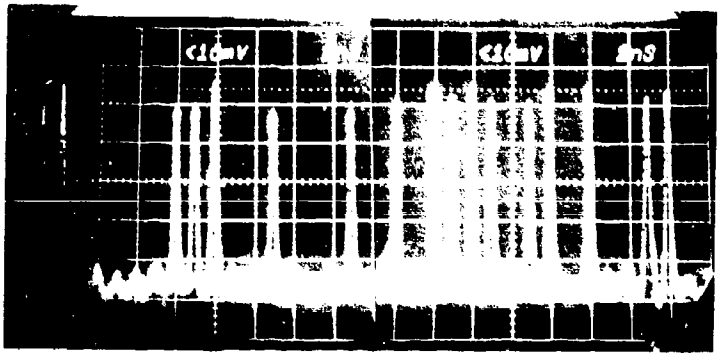

(b) P_1 POLARIZATION
Worst Case Dynamic
Extinction Ratio 7:1

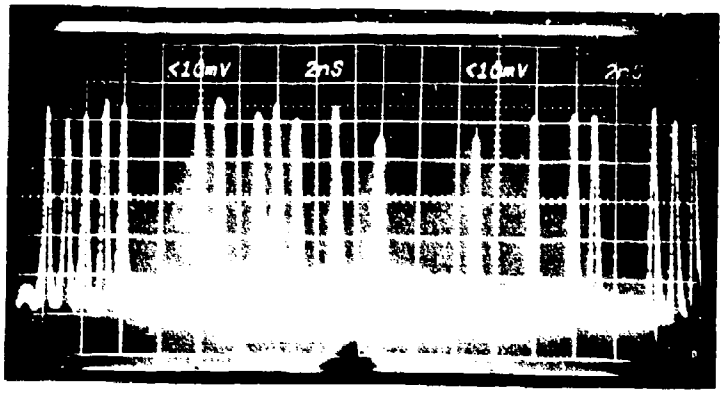

(c) P_2 POLARIZATION
Worst Case Dynamic
Extinction Ratio 9:1

FIGURE 23 1 Gbps PGBM DATA TAKEN USING 24 VOLT MODULATOR (AM #1)
WITH A 24 VOLT DRIVER (SSD #4)

extinction ratio of this modulator. The best 10% to 90% rise times achievable in this program has been about 400 ps to 500 ps with the drivers. These rise times are adequate for the modulator configurations used, provided that the driver is able to maintain timing accuracy to less than $\pm$150 ps.

Since the data was not very good using the SSD #4 driver, it was decided to again use the MD-2-003 driver with better timing accuracy. This decision was made due to the poor dynamic extinction ratio resulting from the poor driver timing accuracy. The timing uncertainties in the MD-2-003 driver was $\leq\pm$200 ps compared to $\leq\pm$350 ps for the SSD #4 driver. Table 6 lists the timing inaccuracies of the one gigabit PN generator and the dual complementary MD-2-003 driver output with respect to the system clock. Figure 24 shows the 1 Gbps driver output and the 31 bit PGBM 1 Gbps detected optical signa. The measured worst case dynamic extinction ratios were 17.5:1 and 22:1 for P_1 and P_2 polarizations respectively. These values were low due to inadequate switching voltage. The reason for the difference between the P_1 and P_2 worst case dynamic extinction ratio is an inherent problem in transistors. It is because when the transistors are turned on the signal reflected from the matching network see 50 ohms impedance at the transistor and is not reflected back to the crystal as when the transistor is off it has a large impedance and reflects the reflected signal causing ripple on driver waveform. Therefore, the two polarizations are different due to driver transistor characteristics. These results were given to show that driver performance will be very critical in Pulse Quaternary Modulation (PQM) where both polarizations are used simultaneously. However, in PGBM one would choose the best extinction ratio output. The peak transmission was only 80% of full amplitude because the zeros were adjusted for the lowest amplitude worst case zero. The laser pulsewidth was approximately 300 ps for these evaluations. This data shows how the dynamic extinction ratio is drastically affected by the timing inaccuracies of the modulator driver output, as the dynamic extinction ratio was improved by better than two with a timing improvement of four-sevenths even though the modulator was underswitching by three-fourths.,

3.2 Modulator (AM #2) With Four 7 mm Long Crystal

This modulator used four crystals optically in series (with a lens between the two pairs) to reduce switching voltage and improve rise time. Figure 25a shows the full 31 bit code output with a 5 ns per division horizontal sweep. Figures 25b and 25c are expanded segments of the code at 2 ns per division. The static extinction ratio of the modulator was poor because crystal work strain was not removed from the crystals by chemical etching. This is a fault of the crystals not being etch long enough for strain removal. Therefore, it was not possible to achieve good dynamic switching performance. In addition, the test laser amplitude fluctuations were 2 dB so that consecutive ones were not of uniform height. The dynamic extinction ratio of this modulator was about 5:1 using the two thin film hybrid front end drivers, MD-2-002 and MD-2-003.

The electrical timing to each crystal was optimized by independently driving each crystal with the other crystal drivers removed. Then all of the crystals were driven simultaneously to achieve full depth of modulation. The decreased crystal capacitance of the 7 mm crystals relieved the rise time problem somewhat, but the crystal capacitance was not the primary limiting factor in the modulator dynamic performance. As mentioned before, we had found that the driver timing accuracy was the limiting factor. Subsequent to the test data shown in Figure 25 the internal crystals and lens alignment in the

TABLE 6. GIGABIT TIMING INACCURACIES FOR THE 18 VOLT THIN FILM HYBRID FRONT STAGE DRIVER (MD-2-003)

TRANSITION	PN DATA INPUT TO MODULATOR DRIVER (ps)	MODULATOR DRIVER OUTPUT (ps) LEFT	RIGHT
1	0 ps	-50 ps	+200 ps
2	+40	0	+200
3	+80	0	+150
4	0	-80	-150
5	+80	+80	+50
6	+100	0	+150
7	+60	-40	0
8	0	-30	0
9	+70	-60	0
10	-20	-60	-80
11	+80	0	+200
12	-20	-80	-100
13	+20	+50	+150
14	-20	+30	0
15	+120	0	+100
16	0	-80	-200

This data was taken with reference to the system clock.

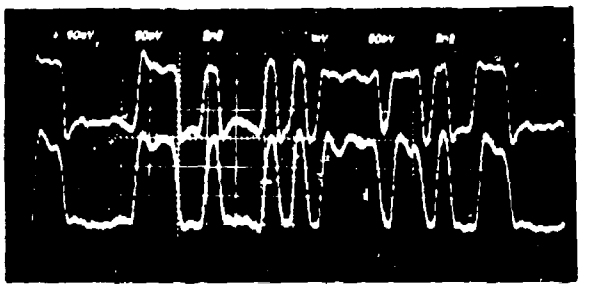

(a) Modulator Driver MD2-002 Output

(b) P_1 Polarization
Worst Case Dynamic Extinction Ratio $\geq$22:1

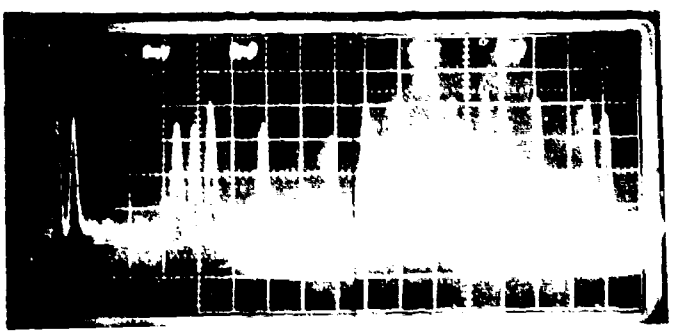

(c) P_2 Polarization
Worst Case Dynamic Extinction Ratio $\geq$ 22:1

FIGURE 24 1 Gbps PGBM DATA TAKEN USING 24 VOLT MODULATOR (AM #1) WITH (MD-2-003) DRIVER AND BETTER PN GENERATOR TIMING ACCURACY INPUT

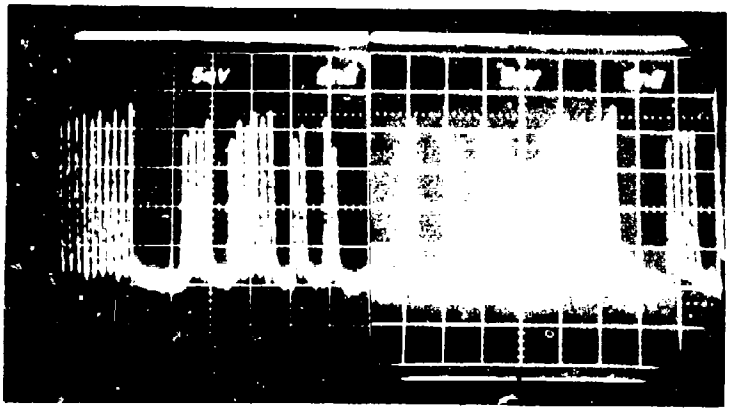

(a) Full Code, 5 nsec/div

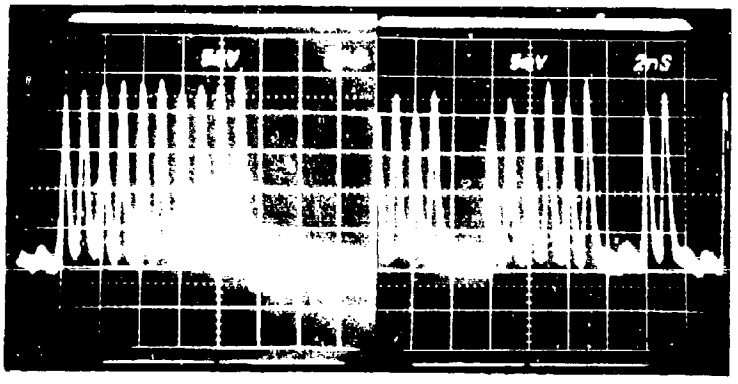

(b) Partial Code, 2 nsec/div

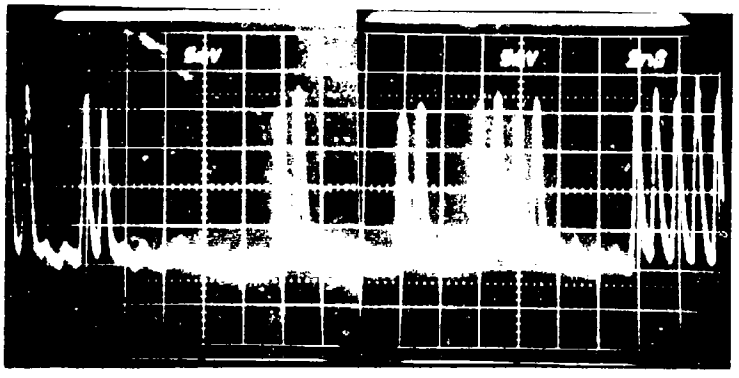

(c) Partial Code, 2 nsec/div

FIGURE 25 1 Gbps PGBM DATA USING FOUR 7mm CRYSTAL MODULATOR (AM #2) WITH 18 VOLT DRIVERS (MD-2-002 and MD-2-003)

breadboard fixture became excessively critical; it was concluded that it would be more productive to spend the remaining program manhours fabricating a modulator with two 10 mm crystals tapered for reduced capacitance or switching voltage, rather than repair the four 7 mm crystal modulator. Although the four crystal modulator had less critical driver timing accuracy requirements due to reduced capacitance, the additional driver added approximately 12 watts of power consumption, and the optical transmission was reduced due to six extra optical surfaces and 50% more crystal length. Since the required laser power was directly proportional to the tranmission losses the two crystal modulator seems to be the better system choice.

Since the two 15 mm crystal would also have the same power consumption, and reduced transmission due to 50% more crystal length it was decided not to fabricate any 15 mm modulators. Also these modulators would require new matching network techniques which consumed a considerable amount of time in previous modulator development programs.

3.3 Modulator (AM #3) With Two 10 mm Crystals Tapered For Capacitance Reduction

Dynamic switching tests of this 10 mm tapered crystal modulator were performed using a 0.53 μm CW krypton laser to observe the optical gate. Figure 26 shows the results of this investigation. The driver used was a thin film hybrid circuit driver operating at 18 volts (MD-2-003). Figure 26a shows the 1010 portion of the code on an expanded scale and Figure 26b shows the 1111 portion of the code. Figure 26c shows the entire code. The optical waveform duplicated the driver waveform with some rounding of the peaks and valleys due to the fall off of the modulator passband at high frequencies. It was noted, however, that the modulator rose to full amplitude proportional to driver amplitude at every transition and that the fidelity of the modulator response was good. The modulator bias was adjusted to be in the linear range since the driver amplitude was 18 volts, while the modulator switching voltage was 24 volts.

It was concluded from these photographs that the modulator driver rise time ($\leq$ 500 ps) was sufficient for use with a 1 Gpps optical pulse train when the laser pulses were no more than 300 ps in length. However, good system performance will require driver timing accuracies less than $\pm$ 150 ps.

This tapered crystal modulator was evaluated using a 1 Gpps optical pulse train made up of two time multiplexed equal amplitude 500 Mpps trains. The driver in this case was the best 24 volt discrete component driver (SSD #4). The 1 Gbps PN data input to the modulator driver had timing inaccuracies of $\leq \pm$ 70 ps reference to the system clock. Figure 27 shows the results of this test. Both polarizations were displayed to indicate full dynamic switching. The worst case bit indicated about 7:1 dynamic extinction ratio. Moving the driver timing in either direction helped some bits and degraded others. The driver waveform, shown in Figure 27, indicated that the driver transitions were $\pm$ 350 ps from the optimum transition point. This implied driver timing inaccuracies of $\leq \pm$ 350 ps. Observation of the worst bits while moving driver timing, indicated that improvement of the driver timing accuracy to $\pm$ 100 ps would improve the dynamic extinction ratio by about a factor of three. The laser pulse width was about 300 ps for this test. The results shown in Figure 27 indicated that the driver-modulator rise time was not the dominating factor in determining the dynamic extinction ratio of the modulator, but that driver timing accuracy accounted for every bad bit.

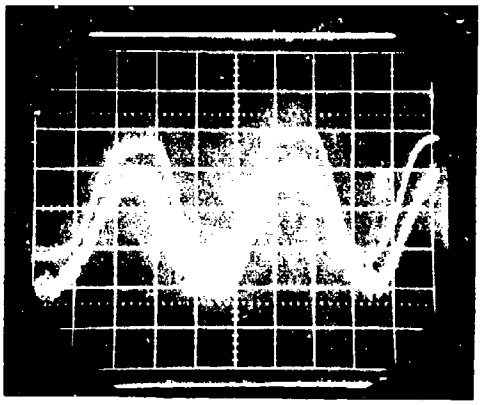

(a) 500 ps/div
Upper Trace -
driver at 5 volt/div
Lower Trace - Optical gate

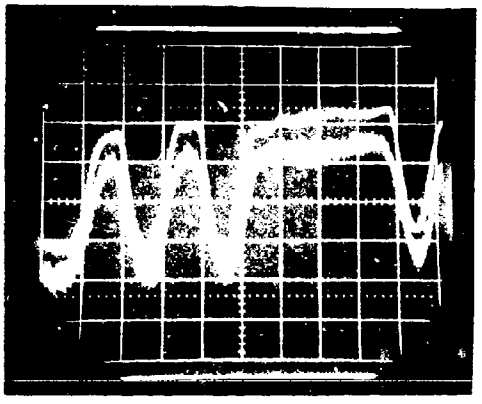

(b) 1 nsec/div
Upper Trace -
driver at 5 volt/div
Lower Trace - Optical gate

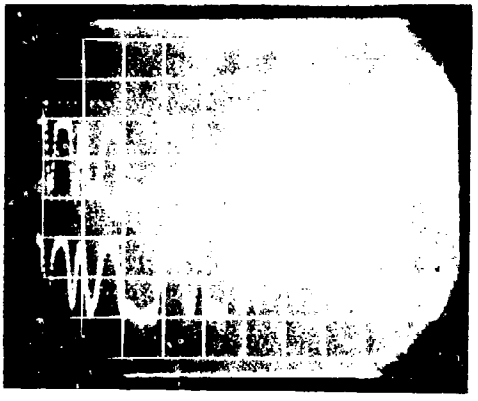

(c) 5 nsec/div
Upper Trace -
driver at 10 volt/div
Lower Trace - Optical gate

FIGURE 26 OPTICAL GATE OF CAPACITANCE REDUCTION TAPERED CRYSTAL MODULATOR (AM #3) USING MD-2-003 DRIVER

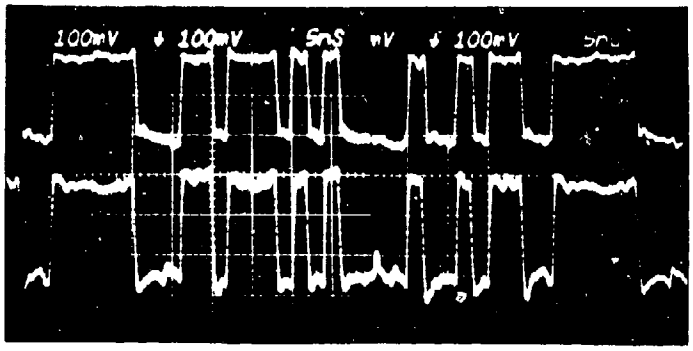

(a) Modulated Driver Outputs

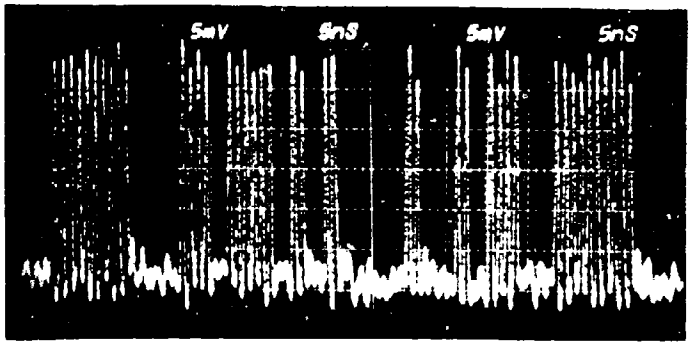

(b) P_1 Polarization
Worst Case Dynamic Extinction Ratio $\geq$ 7:1

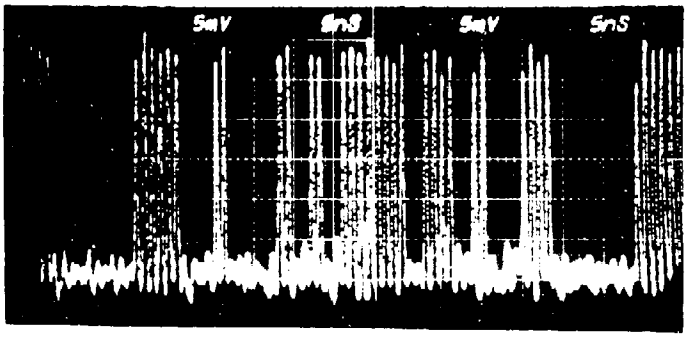

(c) P_2 Polarization
Worst Case Dynamic Extinction Ratio $\geq$ 7:1

FIGURE 27 1 Gbps PGBM DATA USING 24 VOLT TAPERED CRYSTAL MODULATOR (AM #3) FOR CAPACITANCE REDUCTION WITH 24 VOLT DRIVER (SSD #4)

In order to further verify this result the 24 volt straight crystal modulator (AM #1) described in Sections 2.3.1 and 3.1, was operated with the same driver (SSD #4), same PN generator, and under the same optical conditions as those in Figure 27. Figure 28 shows the results of this test. The same results as observed with the tapered crystal modulator were true for this modulator. The worst bit dynamic extinction ratio was about 7:1 and all bad bits were due to driver timing inaccuracies. The same bits were deficient in both cases. The two figures did not correspond exactly bit by bit in amplitude heights because of laser amplitude fluctuations of about 2 dB.

Since it was concluded that the dynamic extinction ratio of the modulator had limitations as the result of driver inaccuracies, it was decided that the best approach to the problem would be to fabricate a modulator which would require a lower half-wave switching voltage. This conclusion was reached because drivers could be built with much less timing inaccuracies if no more than 20 volts of output was necessary since an extra high power amplification stage was required for more power output which further increased the timing inaccuracies.

Further evaluations were not done on this modulator since it was concluded that the remainder of this program would be best spent fabricating a 20 volt modulator and improved 20 volt driver.

3.4 Modulator (AM #4) With Two 10 mm Crystals Tapered For Voltage Reduction

Dynamic switching tests were performed using a breadboard modulator driver (SSD #4), and a CW 0.53 μm Krypton laser in order to observe the optical rise time and switching fidelity. Input to the driver was a 31 bit PN code in NRZ format at 1 Gbps. Figure 29 shows a superposition of the 24 volt discrete component driver output waveform and the modulated light. Because the two modulator crystals were separately matched and a dual output driver was used, the driver output waveform display was obtained by adding the two driver outputs to form one effective output. As shown in the figure there was excellent agreement between the modulated light and driver output. In particular, it was seen that although tapering the crystals for reduced switching voltage also produced a corresponding increase in crystal capacitance, the optical rise time was not limited by the RC time constant of the crystal voltage. Dynamic switching voltage tests were also performed using a mode-locked frequency doubled Nd:YAG laser with an output optically multiplexed to produce a 1 Gpps optical pulse train. The modulator was driven by a dual output modulator driver with thin film hybrid cricuit front stage and discrete component output stages (MD-2-003), operating at 1 Gbps to produce PGBM modulated light at that data rate. This driver, which was capable of switching 18 volts peak-to-peak, was chosen for these mode-locked dynamic tests because it exhibited better timing accuracy ($\leq \pm 200$ ps) than the driver used in the CW laser evaluations ($\leq \pm 350$ ps). The complete 31 bit PN code modulated light output is shown in Figure 30. Although the driver produced only 90% of the required switching voltage, the worst bit dynamic extinction ratio was limited by one particularly bad bit which resulted from a combination of timing errors and lower driver amplitude. Without this one bit the worst bit dynamic extinction ratio for the remainder of the code was 24.6:1. Because these dynamic results were preliminary, further efforts were initiated to improve timing accuracy of this modulator-driver combination with a driver which had 20 volt outputs.

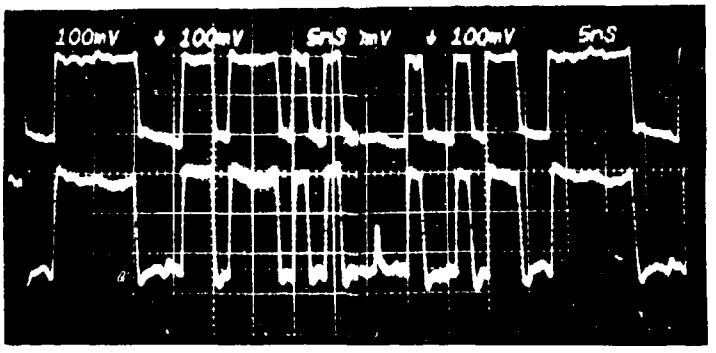

(a) Modulator Driver Outputs

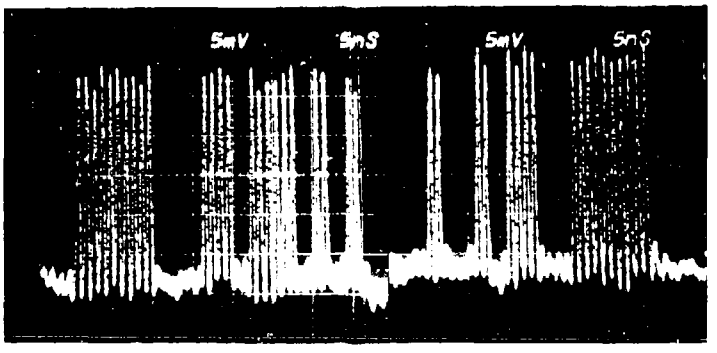

(b) P_1 Polarization
Worst Case Dynamic Extinction Ratio $\geq$ 7:1

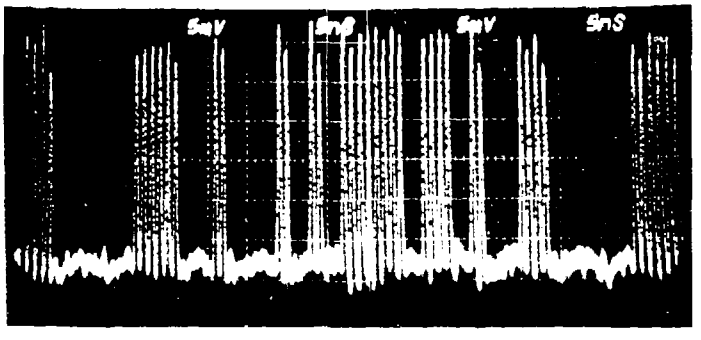

(c) P_2 Polarization
Worst Case Dynamic Extinction Ratio $\geq$ 7:1

FIGURE 28 1 Gbps PGBM DATA USING 24 VOLT CRYSTAL MODULATOR (AM #1) WITH 24 VOLT DRIVER (SSD #4)

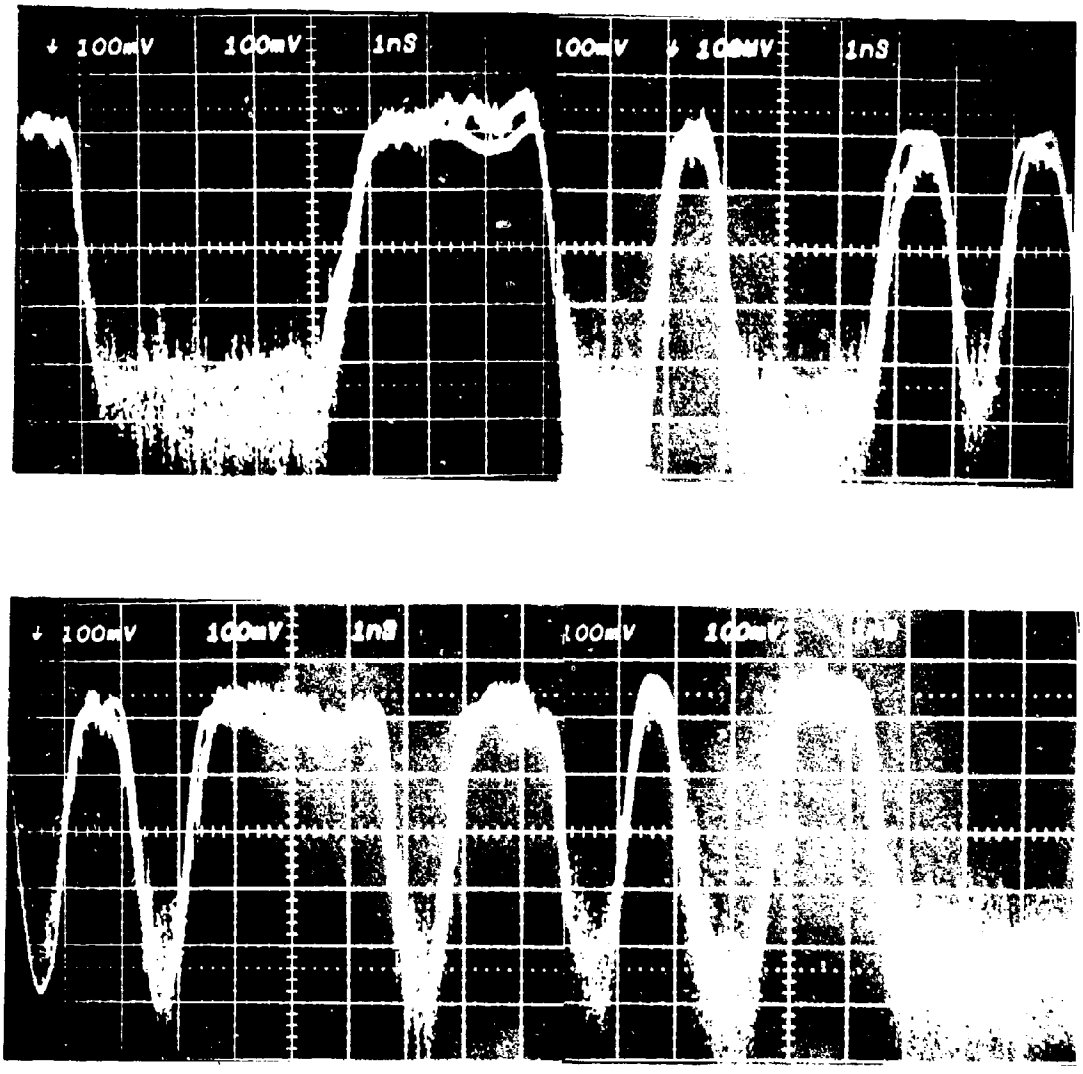

FIGURE 29 1 Gbps NRZ MODULATION WITH VOLTAGE TAPERED CRYSTAL MODULATOR (AM #4) USING 24 VOLT DRIVER (SSD #4)

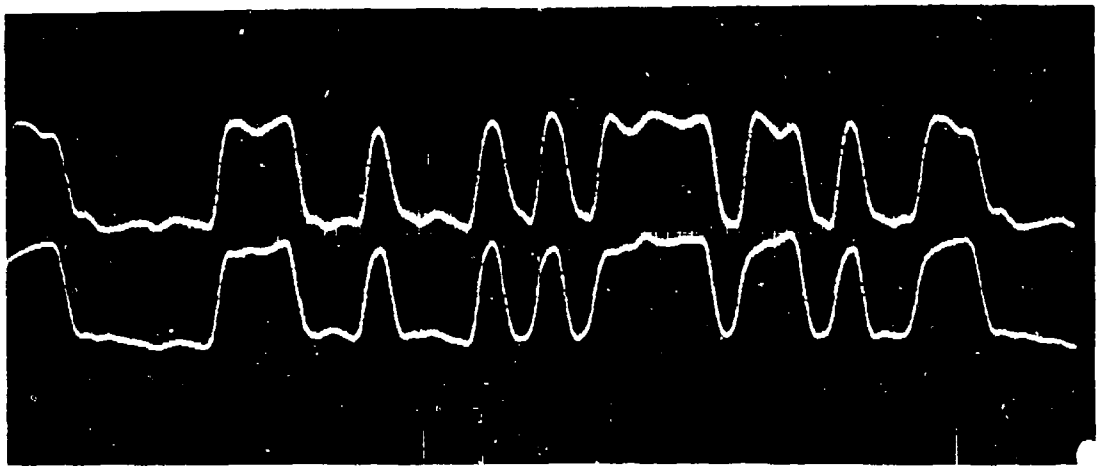

(a) MD2-002 Modulator Driver Output
Vertical Scale 2 nsec/div; Horizontal Scale 10 volts/div

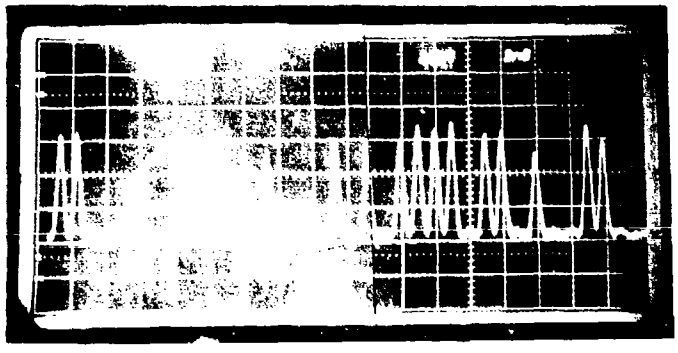

(b) P_1 Polarization
Worst Case Dynamic Extinction Ratio $\geq$ 19:1

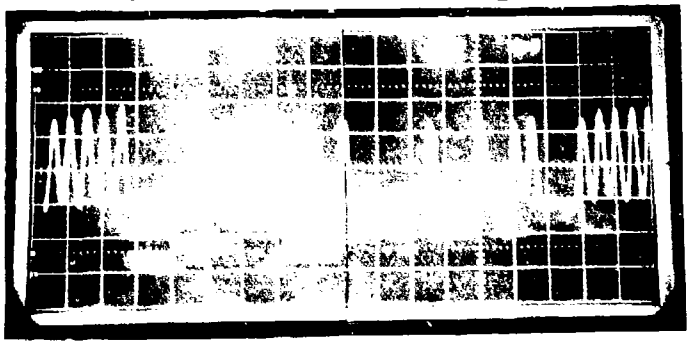

(c) P_2 Polarization
Worst Case Dynamic Extinction Ratio $\geq$ 16.3:1

FIGURE 30 1 Gbps PGBM DATA USING VOLTAGE TAPERED CRYSTAL MODULATOR (AM #4) WITH 18 VOLT DRIVER (MD-2-003)

Dynamic switching voltage tests were performed with the voltage tapered crystal modulator (AM #4) using a 500 Mpps mode-locked and frequency doubled Nd:YAG laser with its output optically multiplexed to produce a 1 Gpps optical pulse train. The modulator was driven by the dual output modulator driver, 3x, operating at 1 Gbps to produce PGBM modulated light at that data rate. Table 7 lists the timing inaccuracies of this driver's two complementary outputs which ranged from -150 ps to +200 ps giving inaccuracies of $\leq \pm$ 175 ps with respect to the system clock. The PN generator had inaccuracies ranging from 0 to +140 ps giving inaccuracies of $\leq \pm$ 70 ps with respect to the system clock. The switching voltage of the two outputs were 20 volts $\pm$ 1 volt and rise times were observed to be between 400 ps and 500 ps. Figure 31 shows the modulator driver output waveform at 10 volts per vertical division and 1 nanosecond per horizontal division. Figure 32 shows the extinction ratios for the entire 31 bit code PGBM data for both orthogonal polarizations, which was denoted as P_1 and P_2 for purposes of identification. Data was obtained by optimizing each polarization separately, since in PGBM the best worst case dynamic extinction ratio polarization would be chosen. The worst case dynamic extinction ratios were $\geq$ 22.4:1 and $\geq$ 23.7:1 for polarizations P_1 and P_2 respectively. The worst case dynamic extinction ratios were possibly better than these values since pickup in the optical detector made it difficult to accurately measure the zero levels. The detector noise pickup had not been seen previously due to high zero levels; now that the zero levels are low the pickup is larger relative to the zeros so it presents a problem in accurately determining the zero heights.

TABLE 7. GIGABIT TIMING INACCURACIES FOR THE 20 VOLT DISCRETE COMPONENT DRIVER (3X)

TRANSITION	PN DATA INPUT TO MODULATOR DRIVER (ps)	MODULATOR DRIVER OUTPUT (ps) LEFT	RIGHT
1	0 ps	-160 ps	0 ps
2	+100	-80	-100
3	+100	-80	0
4	+50	+50	0
5	+120	+120	-50
6	+140	-150	-150
7	+130	+50	0
8	+30	+100	+150
9	+125	+150	+200
10	+100	+100	+100
11	0	-100	+50
12	+30	-100	0
13	0	-160	0
14	+120	-50	0
15	0	0	+100

This data was taken with reference to the system clock.

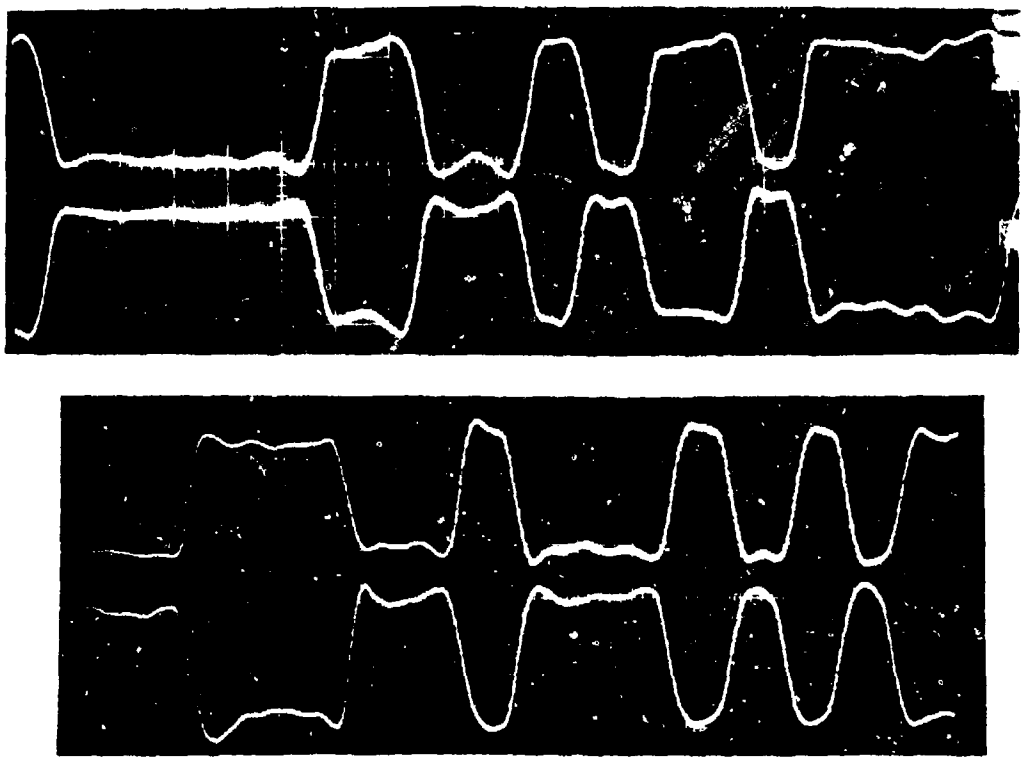

FIGURE 31 1 Gbps PGBM DATA USING VOLTAGE TAPERED CRYSTAL MODULATOR (AM #4) WITH 20 VOLT DRIVER (3x)

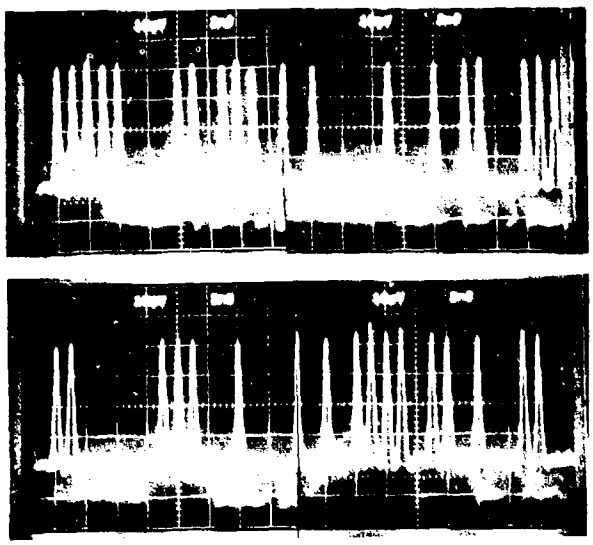

a) P_1 Polarization Worst Case Dynamic Extinction Ratio $\geq$ 22.4:1

b) P_2 Polarization Worst Case Dynamic Extinction Ratio $\geq$ 23.7:1

FIGURE 32 1 Gbps PGBM DATA USING VOLTAGE TAPERED CRYSTAL MODULATOR (AM #4) WITH 20 VOLT DRIVER (3x)

4. RELIABILITY AND MAINTAINABILITY

In July, 1973, a life test was begun using one of the double-pass breadboard modulators used in the 1 Gbps breadboard communication program (Lab Subsystem Performance Evaluation - Air Force contract F33615-72-C-1908). The life test was being conducted on the laser modulator and modulator driver with associated electronics in order to verify that its components would withstand extended operation, and to obtain some quantitative life test data. This modulator, along with its associated electronics, was operated approximately 1000 hours as part of the breadboard program before this life test was initiated. Although this modulator was a double-pass unit with a manual compensator, it was similar enough to present units in both design and electronics to make the test results meaningful.

The life test setup consisted of the double-pass modulator aligned in the output beam of a CW He-Ne laser. The modulator driver used a 500 Mbps pseudorandom code as a signal source. The modulator output beam was incident on a silicon avalanche photodiode (SAPD) in order to display the NRZ modulated waveform. The driver output test point was also displayed for comparison purposes. Photographs of the modulated light and driver test point outputs have been recorded periodically as well as all of the power supply voltages, the oven temperature, and the relative optical transmission of the unit, since the initiation of this test none of the components have been turned off to the present time. This modulator has now operated more than 7385 hours on the life test setup without failure of any modulator component or apparent degradation of the optical output waveform. Figure 33 shows the initial data at zero hours and after continuous operation for 3000 hours. The inherent modulator stability and reliability have been illustrated in this life test by the fact that no adjustments have been required due to aging of components in this modulator unit, and by the consistent data obtained for the measured parameters. The 150°C oven temperature, for example, has varied only 1°C since the beginning of the test. The power supply voltages measured at the beginning of the test and after 3500 hours and 7385 hours are given in Table 8. The voltage changes, ΔV, have been less than 0.76 volts and most were in the tens-of-millivolts range which was the accuracy limit of the meters used to make the measurements. In summary, the life test results to date indicated excellent modulator operation with no signs of degradation and no modulator component failures.

None of the modulators built for this program were subjected to life test, but the same materials and fabrication techniques used in the breadboard modulator were used for these modulators. The 1 Gbps modulators built for this program should actually have better life time capability than the breadboard unit described above because of the use of improved lithium tantalate material, fewer optical surfaces, larger optical safety factor and less critical mechanical alignment requirements (due to the single pass crystal configuration).

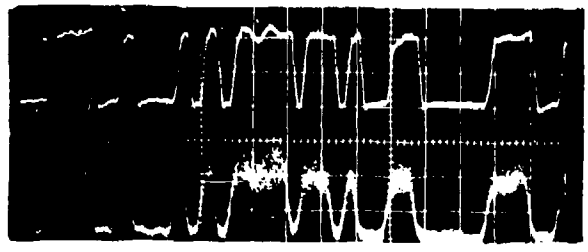

Beginning Data
5 ns/div

Driver Test Point

Modulated Light Signal

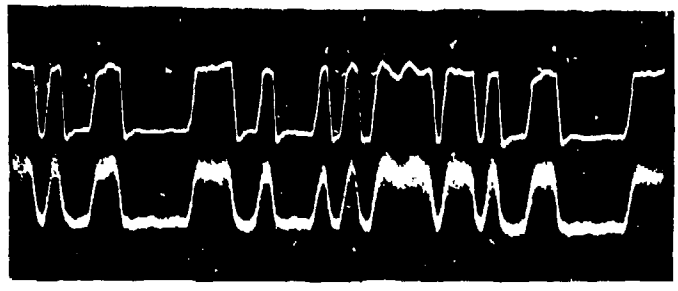

3,000 Hours Data
5 ns/div

Driver Test Point

Modulated Light Signal

FIGURE 33 LIFE TEST DATA
Driver Output and Modulated Light Signal at Beginning of Life Test and After 3000 Hours of Continuous Operation

TABLE 8. LIFE TEST POWER SUPPLY OUTPUT VOLTAGE DATA

VOLTAGE AT 0 HOURS	VOLTAGE AT 3500 HOURS	VOLTAGE AT 7385 HOURS	Δ VOLTS
+ 4.91 volts	+ 4.92 volts	+ 4.93 volts	+0.02 volts
- 5.41	- 5.40	- 5.39	-0.02
+15.20	+15.18	+15.19	-0.01
-15.28	-15.29	-15.31	+0.03
+18.07	+17.99	+17.97	-0.10
+26.20	+26.13	+26.10	+0.10
+20.80	+21.06	+21.02	+0.22
+31.90	+32.28	+32.66	+0.76
-33.50	-33.73	-34.17	+0.64

5. CONCLUSIONS AND RECOMMENDATIONS

A number of modulator and modulator driver improvements were developed during this exploratory program in order to improve overall 1 Gbps PGBM modulator operation. Matching network calculations were done to determine modulator optical response at various crystal capacitances and modulated frequencies. These calculations indicated that a tapered crystal modulator would perform considerably better dynamically than a square crystal modulator. The power spectrum of a 1 Gbps modulator driver was measured and determined that it falls off at about 20 dB/GHz. The 50 ohm termination box used with the crystal matching networks was redesigned and currently reflection coefficients measure less than 4% up to frequencies of 1500 MHz. These loads did not degrade modulator driver performance. The calculated effect of modulator driver timing error on the dynamic extinction ratio for 1 Gbps operation allowed little timing error (160 ps) for driver rise times of 500 ps with a laser pulse width of 300 ps, for a dynamic extinction ratio of 10:1. It was shown that a decrease in the driver rise time produced a corresponding increase in allowable timing error. The crystal transit time used in these calculations was 75 ps.

The best dynamic modulator performance achieved in this program was taken using a dual output discrete component driver with 20 volts $\pm$ 1 volt output having timing inaccuracies of $\leq \pm$ 175 ps including the 1 Gbps PN data generator which had timing inaccuracies of $\leq \pm$ 70 ps. The driver had rise times between 400 ps and 500 ps. The modulator used was the two 10 mm long voltage tapered crystal modulator which required 19.8 volts for full half-wave switching. The modulator transmitted 81.5% of the laser beam input power statically. The amplitude of the smallest "one" was 95.5% of the maximum "one" transmission, therefore the dynamic transmission of the smallest "one" was 78%. The worst case dynamic extinction ratio for this modulator and modulator driver combination was $\geq$22.4:1 with a 1 Gbps pseudorandom 31 bit code input. These evaluations were only done at low optical power levels (< 10 mW) due to unavailability of a high optical power mode-locked frequency doubled Nd:YAG laser. However, no apparent degradation was seen in optical performance for the brassboard modulators at high optical power levels as noted in the Laser Modulator II program (F33615-73-C-1038); therefore, due to the use of similar high purity lithium tantalate and fabrication techniques, it is expected that an equal performance could be achieved.

Reliability and maintainability tests of a modulator and modulator driver with associated electronics similar to these fabricated in this program had shown no noticeable degradation in the modulator electronics in a life test setup over a period of 7385 hours plus 1000 hours in which it was used in breadboard evaluation. The 1 Gbps modulators fabricated for this program should actually have better lifetime capability than the double-pass breadboard unit described above because of the use of improved lithium tantalate material, fewer optical surfaces, larger optical safety factor, and less critical mechanical alignment requirement.

The program was very successful and significant improvements were made. However, two problem areas remain. First, the modulator transmission was lower than desired; however, it is believed that better crystal optical polishing of the faces, better crystal cleaning preparation before AR coating, and improved AR coating techniques will greatly improve the overall transmission of the modulator. Keimpe Andringa of Raytheon had measured surface losses for AR coated laser windows of less than 0.1% from a number of vendors. Therefore, with proper fabrication techniques better than 80% transmission is predicted for future modulator units. Second, dynamic performance of the modulator was limited by driver timing inaccuracies; however, it is believed that with better timing accuracy in the PN data generator and faster transistors for the modulator driver, the modulator driver timing inaccuracies could be improved by as much as 50 ps.